2016

Dcbld2/esdn Is Essential For Proper Optic Tract Formation And Retinal Lamination

Ryan Mears Joy
University of Vermont

DCBLD2/ESDN IS ESSENTIAL FOR PROPER OPTIC TRACT FORMATION AND RETINAL LAMINATION

A Thesis Presented

by

Ryan Joy

to

The Faculty of the Graduate College

of

The University of Vermont

In Partial Fulfillment of the Requirements
for the Degree of Master of Science
Specializing in Biology

May, 2016

Defense Date: January 7, 2016
Thesis Examination Committee:

Bryan A. Ballif, Ph.D., Advisor
Jason Stumpff, Ph.D., Chairperson
Alicia M. Ebert, Ph.D.
Paula Deming, Ph.D., MT
Cynthia J. Forehand, Ph.D., Dean of the Graduate College

ABSTRACT

The Discoidin, CUB and LCCL domain-containing protein 2 (DCBLD2/ESDN/CLCP1) is a type-I, transmembrane receptor that mediates diverse cellular processes such as angiogenesis, vascular remodeling, cellular migration and proliferation. Identification of DCBLD2 in a proteomics screen to identify substrates of Src family tyrosine kinases that bind the Src homology 2 domain of CT10 regulator of kinase-Like (CrkL), a critical scaffolding protein for neuronal development, led to a need for further characterization of the protein. To elucidate the role of this interaction and potential novel function of DCBLD2, an *in vivo* approach utilizing *Danio rerio* (zebrafish) was conducted. dcbld2 was found localized in neuronal tissues during development, with strong expression in the retina. Knockdown of the protein led to a deficiency of retinal ganglion cells and the optic tracts, or nerve bundles, they project to innervate the brain. Serial sections revealed malformation of the normally discrete layering of retinal cell types, and smaller eye area overall.

These findings suggest a role for dcbld2 in developing nervous tissue, specifically neuronal migration during interkinetic nuclear migration. While it is has been shown that dcbld2 has a role in the developmental patterning of intersegmental vessels in the tail of zebrafish, the protein has not been investigated in the context of neurogenesis. The loss of RGCs and lamination defects observed in the eye, along with its association with the CrkL-SH2 domain, implicate it in processes that allow for the proper differentiation of neurons. This study has brought us further down the path to understanding the multiple functions of the receptor; however, further studies are required to delineate the exact mechanistic function of the dcbld2 receptor.

ACKNOWLEDGEMENTS

I would like to thank my advisor, Dr. Bryan Ballif, for his humor, ping pong competitiveness, undying patience, kindness, and most importantly his dedication to see all of his students succeed. His motivation and determination have made it possible for me to complete this thesis.

Gratitude is also extended to Dr. Alicia Ebert who guided me through the techniques and protocols of the *in vivo* portion of this thesis. I have appreciated Dr. Ebert's ability to be frank and her get-it-done attitude which culminates in her lab having a strong working environment. Dr. Ebert's willingness to share her knowledge and work with students outside her purview speaks volumes about her as a person.

My other committee members, Dr. Jason Stumpff and Paula Deming, have also been crucial in seeing me through to this point. Their flexibility and thoughtfulness has allowed me to refine my goals as a student and determine the career path that I want to walk.

Lastly, I would like to thank my wife, Kathryn, who has seen me through thick and thin, and is always there when I need support. Her ability to see the big picture and help me to do the same has improved my life from the time that she entered it.

This work was supported by U.S. National Science Foundation IOS grants 1021795 and 1456846, the Vermont Genetics Network through U. S. National Institutes of Health Grant 8P20GM103449 from the INBRE program of the NIGMS, and U.S. National Institutes of Health Grant 5P20RR016435 from the COBRE program of the NIGMS.

TABLE OF CONTENTS

Page

LIST OF FIGURES

Figure Page

ABBREVIATIONS

BMP: Bone morphogenetic protein

C3G (RAPGEF1): Rap1 guanine nucleotide exchange factor

CDCP1: Cub domain containing protein 1

Crk/L: Crk family adaptor proteins

Crk: CT10 regulator of kinase

CUB: Compliment C1r/C1s, Uegf, Bmp1 domain

Dab1: Disabled-1

DCBLD2/ESDN/CLCP1: Discoidin, cub, and LCCL domain containing protein 2

EF1α: Elongation factor 1 alpha

Erk: Extracellular regulated tyrosine kinase

EtOH: Ethanol

FGF: Fibroblast growth factor

FYN: Src family tyrosine kinase

Fz-LRP: Frizzled-low density lipoprotein receptor

GO: Gene ontology

H+E: Hematoxylin and eosin histological stain

HPF: Hours post fertilization

Hu: Homo sapien (human)

INL: Inner nuclear layer

IPL: Inner plexiform layer

Isl2b:GFP: Transgenic zebrafish line with fluorescent RGCs

LCCL: Limulus clotting factor C, Coch-5b2, and Lgl1 domain

MeOH: Methanol

Mm: Mus musculus (mouse)

N-cad (CDH2): Neural cadherin-2

ONL: Outer nuclear layer

OPL: Outer plexiform layer

PBS: Phosphate buffered saline

PBT: Phosphate buffered tris

PDGF: Platelet derived growth factor

PFA: Paraformaldehyde

pY: Phosphotyrosine

RA: Retinoic acid

RGC: Retinal ganglion cell

Rn: Rattus norvegicus (Norway rat)

RPC: Retinal precursor

RPE: Retinal pigmented epithelium

SEMA4B: Semaphorin 4B

SFK: Src family tyrosine kinases

SH2: Src homology 2 domain

SH3: Src homology 3 domain

SHH: Sonic hedgehog growth factor

SILAC: Stable isotope labeling in cell culture

Src: Tyrosine kinase (sarcoma)

SSC: Saline-sodium citrate

Tr: Takifugu rubripes (tiger puffer fish)

UIC: Un-injected control

VEGF: Vascular endothelial growth factor

VSMC: Vascular smooth muscle cells

WCE: Whole cell extract

Wnt: Wingless/int-1 protein

YSL: Yolk syncytial layer

REVIEW OF THE DCBLD2 RECEPTOR

DCBLD2 Receptor

The discoidin, cub, and LCCL domain containing protein 2 (DCBLD2/ESDN/CLCP1) is a type-I, or single pass, transmembrane receptor with an intracellular C-terminus. The receptor was first identified in coronary arterial cells by a group investigating the cellular players in arterial transplant rejection. Smooth muscle migration is a major contributor to transplant rejection, also known as graft arteriosclerosis, as blockage of the artery by newly positioned vascular smooth muscle cells (VSMC) can compromise transplant procedures (Figure 1.1.0 B). *DCBLD2* was found to be upregulated in migrating VSMCs after induced injury (Kobuke, Furukawa et al. 2001). Immunohistological staining showed that *DCBLD2* expression was not only upregulated in remodeling tissues, but localization on the inner layer of the artery was consistent with the localization of migrating smooth muscle cells (Kobuke, Furukawa et al. 2001). DCBLD2 was also suggested to be involved with proliferation as Bromodeoxyuridine (BrdU) uptake in DCBLD2 transfected cells was reduced (Kobuke, Furukawa et al. 2001). Lastly, Dcbld2 expression was evaluated in rat and it was found to ubiquitous, except in liver and whole blood (Kobuke, Furukawa et al. 2001) (Figure 1.1.0 A). The highest expression levels, other than in VSMCs, were found in the brain and heart (Kobuke, Furukawa et al. 2001) (Figure 1.1.0 A).

The Sadeghi group recapitulated this study in coronary arteries, confirming the results of the first study and delving further into the signaling components involved.

Inhibition of DCBLD2 was again shown to increase platelet derived growth factor (PDGF) induced VSMC migration and proliferation (Sadeghi, Esmailzadeh et al. 2007). Furthermore, phosphorylation levels on both the Erk1/2 and Src kinases, which are involved in migration and division, increased when DCBLD2 was knocked down (Guo, Nie et al. 2009). DCBLD2 was also shown to modulate signaling coming from vascular endothelial growth factor (VEGF) in an inhibitory fashion (Guo, Nie et al. 2009; Sadeghi, Esmailzadeh et al. 2007). DCBLD2 function cannot be completely resolved, but these results do support a role for DCBLD2 in the signaling events that regulate proliferation and migration.

DCBLD2 was first coined endothelial and smooth muscle derived neuropilin like protein (ESDN), as it was first isolated from endothelial and smooth muscle cells and had a structure reminiscent of neuropilins. Neuropilins are primarily co-receptors for the plexin receptor family in axonal guidance. While the domains of DCBLD2 can vary depending on species, most species carry three domains; a discoidin repeat domain known as a factor V/VIII domain, a cub domain, and a LCCL domain. The factor V/VIII domain will bind anionic phospholipids on platelets and endothelial cells, and is well characterized in the vasculature field for its role in coagulation (Vogel, Abdulhussein et al. 2006). The CUB (complement C1r/C1s, Uegf, Bmp1) domain is a 110 amino acid domain that is found specifically in transmembrane and extracellular proteins. It has been identified in many developmentally important proteins that are involved in functions that include developmental patterning, tissue repair, axon guidance, and angiogenesis (Bork and Beckmann 1993). The LCCL domain is approximately 100 amino acids and is

named for the proteins in which it has been found including Limulus clotting factor C, Coch-5b2, and Lgl1. It has been found to interact with CUB domains and it is also proposed to be involved in lipopolysaccharide binding (Trexler, Banyai et al. 2000), although it has not been well characterized. Overall, the domain complement of the DCBLD2 lends great flexibility to the receptor and could allow it to play multiple roles in cell proliferation or migration settings, primarily as it may be activated by a diversity of ligands.

DCBLD2 was found to have strong overall expression in the brain and found expressed specifically in the cranial nerves and nerve bundles surrounding the carotid artery (Kobuke, Furukawa et al. 2001) . Evidence for DCBLD2 function within the vasculature was clear, but dual role receptor ligand pairs are not uncommon in a developmental context. Ephrin receptors (Ephs) and ephrins are one such couple and a good developmental example. The different ligand receptor isoform combinations are direct patterning of endothelial cells to become venous or arterial during embryogenesis (Wang, Chen et al. 1998). Ephs and ephrins also play roles in nervous tissue development, being involved in notochord development and segmentation of brain regions (Palmer and Klein 2003). The semaphorin and plexin families also fit this niche. Largely driving cell movements, the families are critical for axonal guidance during embryogenesis (Kruger, Aurandt et al. 2005), and semaphorin plexin interactions have been implicated in the movement of endothelial cells to pattern the vasculature (Kruger, Aurandt et al. 2005). Indeed, semaphorin 4b (SEMA4B) has been shown to be a binding partner for DCBLD2 (Nagai, Sugito et al. 2007) (Figure S3). This interaction suggests

that DCBLD2 could be involved in signaling cascades that control cell movements.

DCBLD2's Association with the CrkL-SH2 domain

Supporting the idea of the DCBLD2 having roles in migration and proliferation, was the discovery of DCBLD2 in association with the Src homology domain 2 (SH2) of the CT10 regulator of kinase-like (CrkL) adaptor protein (Aten, Redmond et al. 2013). CrkL is critical for migration processes that pattern the brain. During cerebral cortex development, neuronal precursors migrate along processes in a progression known as interkinetic nuclear migration. As the precursors migrate between the apical and basal surfaces they are continually progressing through the cell cycle. When a precursor undergoes asymmetrical division one of the daughter cells will differentiate based upon its internal constituents (intrinsic) and its environment (extrinsic). Because migration is linked to cell cycle, and environment plays such a large role in cell fate, appropriate migration is critical to the formation of a properly laminated brain and functional synapses.

DCBLD2's interaction with the CrkL-SH2 domain is facilitated by CrkL-SH2 binding motifs (Aten, Redmond et al. 2013). CrkL-SH2 domains will preferentially bind phosphorylated tyrosine residues in a specific motif with a tyrosine in position one and a proline in position four (YxxP). DCBLD2 has seven intracellular CrkL-SH2 binding motifs. Cellular phosphorylation of these motifs has been shown to induce binding of the CrkL-SH2 domain to DCBLD2 (Aten, Redmond et al. 2013). Furthermore, when tyrosine residues in these motifs are mutated stepwise in order of binding probability, the binding

capability of DCBLD2 is reduced. Upon mutation of all seven sites, DCBLD2 no longer shows inducible binding to the CrkL-SH2 domain (Aten, Redmond et al. 2013).

Additionally, it has been shown that the SFK, FYN can phosphorylate DCBLD2 in YxxP motifs and thereby induce its binding to DCBLD2 (Aten, Redmond et al. 2013) (Figure S3). However, the blocking of SFKs with a potent and specific inhibitor sho(Feller 2001)(Feller 2001)ws that while SFKs are sufficient, they are not required for DCBLD2 phosphorylation in YxxP motifs (Aten, Redmond et al. 2013). Kinases outside of the SFKs are able to phosphorylate DCBLD2 as well, and while it has not been shown, presumably induce binding of DCBLD2 to the CrkL-SH2 domain. Kinases involved in DCBLD2's phosphorylation will have to be more fully characterized to gain a better understanding of the pathways it is involved in.

The significance of DCBLD2's association with CrkL is highlighted by the Reelin signaling cascade which mediates cellular migrations during brain development. Reelin, a secreted ligand, binds to its receptors VLDLR and ApoER (Arnaud, Ballif et al. 2003). Disabled-1, now bound to the Reelin receptors, is tyrosine phosphorylated on the intracellular sides by Src family kinases (SFKs) (Curren and D'Arcangelo, 1998).When Dab-1 is tyrosine phosphorylated by SFKs, this allows the Src-homology 2 (SH2) domain of Crk and CrkL to bind (Park and Curran 2008). The Reelin signal is propagated by the constitutive binding of the guanine nucleotide exchange factor (GEF) C3G to the SH3 domain of CrkL and its subsequent tyrosine phosphorylation of SFKs (Ballif, Arnaud et al. 2004). C3G is then able to activate the GTPase Rap1, which can mediate cytoskeleton changes such as integrin-mediated adhesion and cell migration (Ballif, Arnaud et al.

2004). If critical players in this pathway, like Crk and CrkL, are knocked out, cortical lamination is disrupted and, in mice, a Reeler phenotype emerges. This phenotype is characterized by a loss of proper cerebral cortex lamination and a deficient or absent cerebellum (Feller 2001). Due to loss of the cerebellum, the knockout mice have motor control problems and reel from side to side, hence the name of the ligand. The reelin pathway shows the importance of cellular migration pathways in proper nervous tissue development and highlights the CrkL adaptor protein's simple, but critical role in transducing the signal within this cascade.

DCBLD2's interaction with the CrkL-SH2 domain contributes to a block of evidence suggesting a role for DCBLD2 in cellular migration and nervous tissue development: *DCBLD2* is upregulated in motile cells, has been shown to interact with cellular guidance molecules, and modulates cell migration in response to growth factors. *DCBLD2*'s expression in brain and other nervous tissues coincides with the CRKL adaptor's function in neuronal development and patterning. However, a functional role for DCBLD2 in developing neuronal tissues is lacking. Addressing this deficit is a major outcome of the research presented and discussed in sections 1.4 and 1.5 of this thesis.

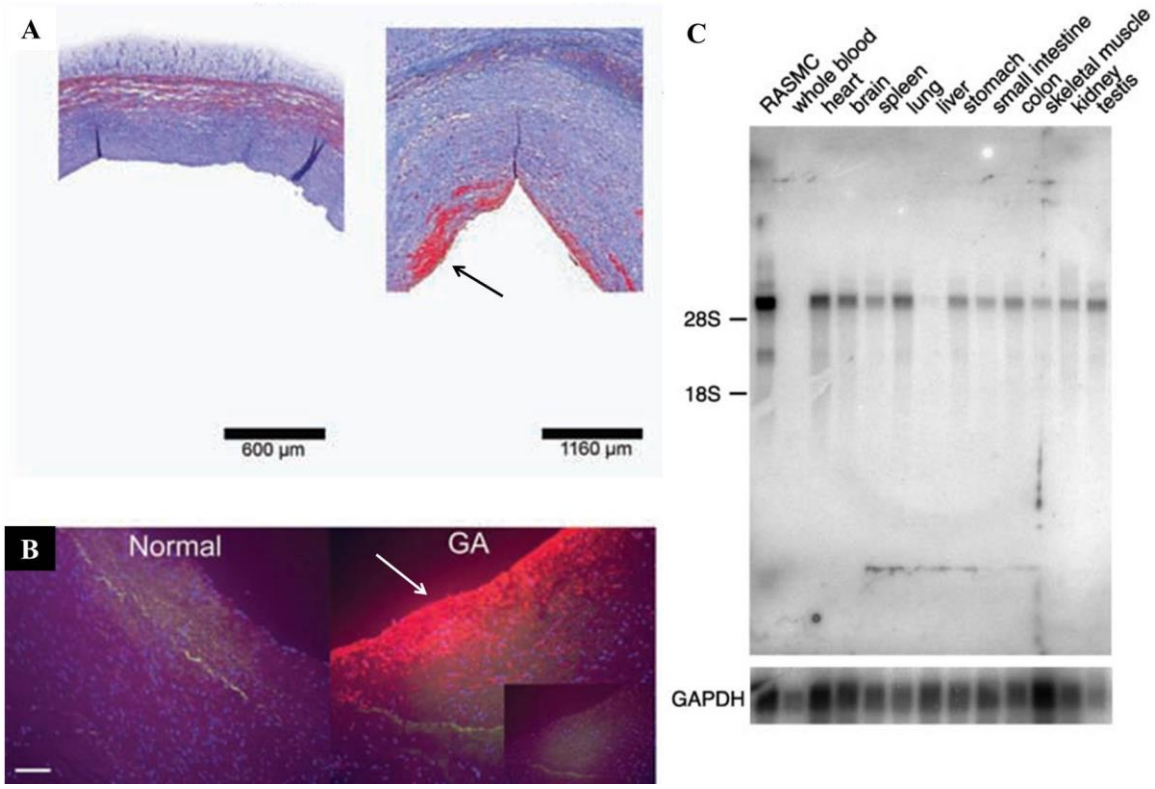

Figure 1.1.0. *Dcbld2* is upregulated after vascular remodeling, and is expressed at high relative levels in the heart and brain. Trichrome stain (red: muscle, blue: collagen) highlighting remodeling smooth muscle forming the neointima (arrows) in normal coronary arteries (A: left panel) and arteries with graft arteriosclerosis (A: right panel). Immunofluorescent staining for Dcbld2/Esdn (B: red signal). Northern blot analysis of Dcbld2 expression in rat organs shows that the receptor is expressed in most organs except liver and whole blood, with strong expression in the heart and brain (C). Adapted from Kobuke, Furukawa et al. 2001, Sadeghi, Esmailzadeh et al. 2007. Permissions granted by the American Society for Biochemistry and Molecular Biology and John Wiley and Sons, license number: 3796020244729.

Zebrafish dcbld2

To more comprehensively explore the function of the human DCBLD2 protein in the developing nervous system in a physiologically-relevant setting, research moved to an *in vivo* model system. The work done on DCBLD2 in vasculature was primarily completed in rodent models given they were mammals and were more amenable to working on vessels and arteries than smaller organisms. The research described in this thesis utilizes the zebrafish model system. The zebrafish model system offers a unique set of properties that allow for strong characterization of developmental genes and proteins. Zebrafish produce an abundance of offspring in a single mating or clutch. Being externally fertilized, the embryos are easy to access and manipulate. Embryos are translucent through most of development and can have their pigment development inhibited easily with phenyl thiourea. Fewer ethical concerns are raised compared to other model vertebrate systems. Zebrafish have strong gene conservation with mammals, including humans. Lastly, the zebrafish eye is ideal for studying developing nervous tissues as it develops quickly and is relatively large.

Due to the value of this system in studying the visual system, multiple eye-specific transgenic lines have been developed and are a powerful tool. Fluorescent tags are cloned behind promoters whose activation marks the birth or differentiation of certain cell types. For example, the *TG(Isl2b:GFP)*^{zc7} (*Isl2b:GFP*) line confers green fluorescence to retinal ganglion cells, rohon-beard neurons, and cranial ganglia when differentiation of these cell types occurs (Pittman, Law et al. 2008). The *TG(Ola:Rx3:GFP)* (*Rx3:GFP*) is another transgenic often used in developmental

investigations, as it labels retinal precursor cells (Brown, Keller et al. 2010). However, it is readily apparent that the protein of interest needs to be expressed in the model system in order to study it. DCBLD2 is not only conserved from human to zebrafish, but across many species (Sievers, Wilm et al. 2011) (Figure 1.1.1) DCBLD2 is 74.8% similar and 53.9% identical between humans and zebrafish at the amino acid level (Sievers, Wilm et al. 2011) (Figure 1.1.1). Crk and CrkL are 82.9% and 94.2% similar, and 70.5% and 82.1% identical, at the amino acid level (Sievers, Wilm et al. 2011) (Figure 1.1.1). Importantly for our purposes, the CrkL-SH2 binding motifs are completely conserved with regard to the critical tyrosine in the first position and proline in the fourth position (Sievers, Wilm et al. 2011) (Figure 1.1.1).

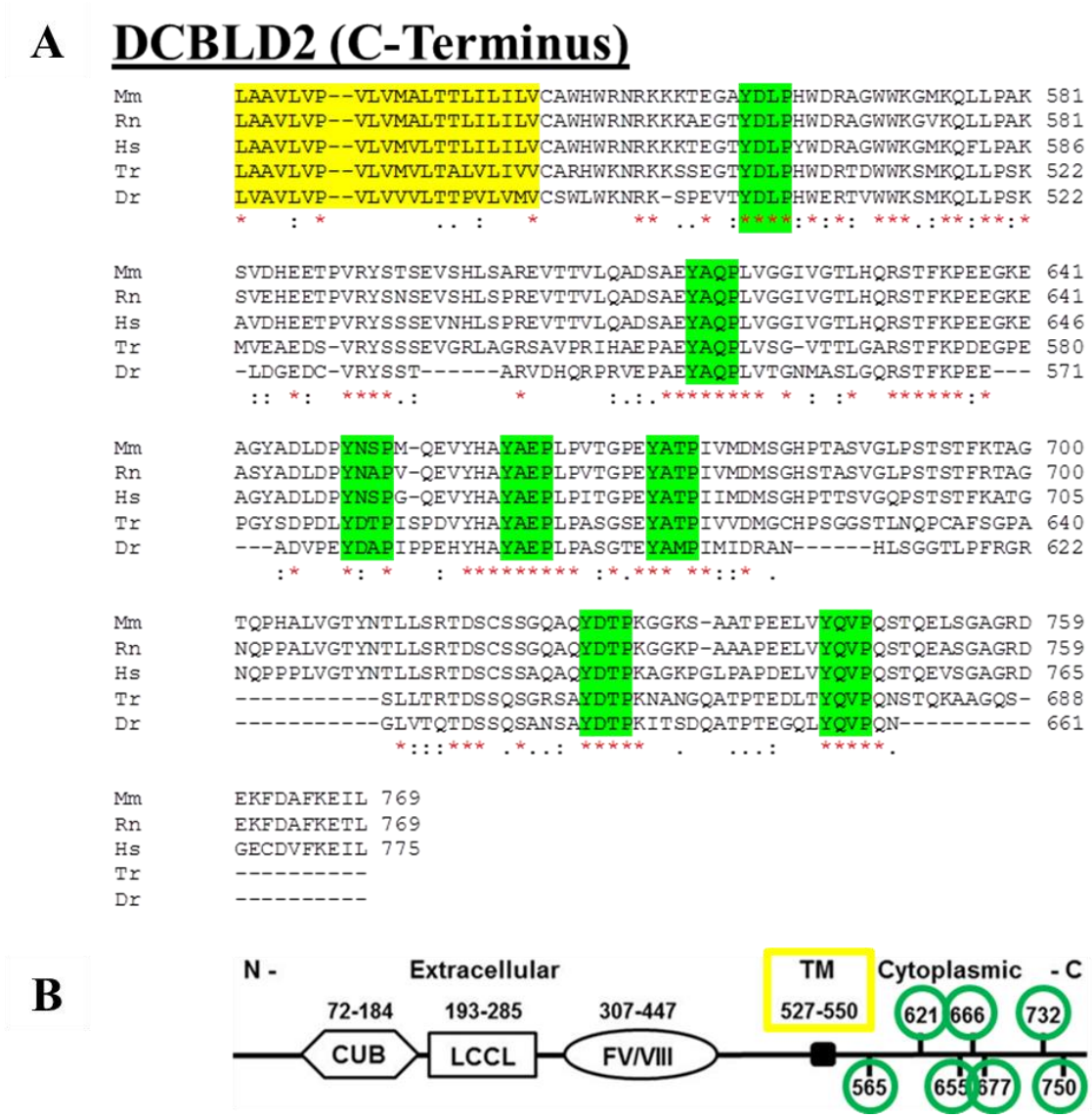

Figure 1.1.1. DCBLD2 is well conserved across vertebrate taxa. Alignment of the C-terminus (T of DCBLD2 primary sequence coming from mouse (Mm), rat (Rn), human (Hs), puffer fish (Tr), and zebra fish (Dr) (A). The entire DCBLD2 sequence is 38.1% conserved across the five species and 19.9% identical. The sequence similarity between zebra fish and human is more striking, being 74.8% similar and 53.9% identical. The seven CrkL-SH2 binding motifs (green, green circles) are 100% identical with regard to the critical 1st and 4th positions in all species (A, B). The transmembrane domain is shown in yellow. Multiple sequence alignment was performed in Clustal Omega (Sievers, Wilm et al. 2011).

REVIEW OF ZEBRAFISH NERVOUS TISSUE DEVELOPMENT

Early Zebrafish Development

Zebrafish nervous tissue development begins after a number of well-orchestrated events induce gastrulation in the embryo and generate the three primary germ layers. Leading up to gastrulation the embryo must undergo a number of cell divisions and coordinated cell movements to orient tissues and signaling molecules for proper entry into gastrulation. Outlined below is a very brief synopsis of zebrafish development up until gastrulation and development of the presumptive neural tissue. Due to the nature of this in nervous tissues, more emphasis is placed on gastrulation and eye genesis.

Zebrafish develop very rapidly, with fertilization-stimulated calcium waves initiating contraction of the actin cytoskeleton after only 10 minutes (Gibson 2014). During the one cell zygote stage, cytoskeleton pressure streams yolk-free cytoplasm, or ooplasm, to the animal pole where it will aggregate to become the blastodisc (Gibson 2014). The blastodisc is the site of the first cell division, transitioning the embryo from the zygote stage to the cleavage stage. The entirety of the embryo will originate from this layer of early dividing cells (blastomeres, blastoderm) atop the yolk, and this subset of meroblastic division is known as discoidal (Gibson 2014). The large, yolk filled cell that sits underneath the blastoderm is the animal pole and provides the nutrients for the developing embryo. After the first cell division, the embryo enters the cleavage stage in which rapid divisions occur synchronously (Kimmel, Ballard et al. 1995).

The blastula stage begins close to the tenth cell division or two hours post

fertilization (hpf). Cells begin to divide asynchronously and more slowly, the embryo begins to use its own genome to create protein products (zygotic transition), and large cell movements can be seen. The midblastula transition is marked by the formation of three distinct cell populations; the yolk syncytial layer (YSL), the enveloping layer (Dievler), the deep cells. The YSL plays a crucial role in guiding cell movements during gastrulation, the EVL will form the periderm; a protective epithelial sheet that will be shed later in development, and the deep cells which will give rise to the embryo itself (Gibson, 2014).

By 6 hours (50% epiboly or shield stage) the zebrafish has entered into gastrulation in which the cells form into the three primary germ layers above the remaining yolk known as the ectoderm, mesoderm, and endoderm. The cells within these layers are now generally fated. Ectoderm derivatives include the nervous system, skin, and teeth. The mesoderm layer forms the muscle of the body, connective tissue, and both blood and blood vessels. The endoderm becomes the respiratory system and the gastrointestinal tract. Post-gastrulation the zebrafish enters segmentation in which the dorsal and ventral ends are developed with their respective structures. The 24-48 hpf period is known as pharyngula, wherein fins begin to develop and the embryo starts to become pigmented. Zebrafish embryos hatch from a membranous shielding known as the chorion between 48 and 72 hpf and enter the larval stage. Larva increase in overall size and grow teeth throughout the larval stage, becoming juvenile from 30-44 dpf. The fish continue to grow and are breeding adults at 90 dpf (Kimmel, Ballard et al. 1995).

Zebrafish Eye Field Specification

The eye is composed of tissues that are first apparent after gastrulation. The retina forms from the neural ectoderm, the cornea and sclera arise from the retinal pigmented epithelium, and the lens is born from the surface ectoderm (Sernagor, 2006). Eye field specification begins with gastrulation and the signaling that mediates the formation of the germ layers.

In zebrafish, gastrulation is marked by a process known as epiboly in which the blastoderm spreads down and around the yolk. As the blastoderm reaches the margin it folds under itself, a process known as involution, running anteriorly, back toward the animal pole, and in doing so creates two layers, the epiblast and hypoblast (Gibson, 2014). The actual mechanism of hypoblast generation is disputed, but it is clear that it is formed on the presumptive dorsal side of the embryo. At the junction of epiblast and hypoblast on the dorsal side of the embryo the embryonic shield is formed. This structure has organizing capabilities and can dictate dorsal ventral axis patterning in the zebrafish (Gibson, 2014). The hypoblast layer of the embryonic shield comes together at the midline and extends anteriorly to form the precursor to the notochord the chordamesoderm (Gibson, 2014). The hypoblast layer will eventually form the mesoderm and the endoderm. The epiblast layer also converges toward the midline and extends anteriorly, and is layered above of the hypoblast. This movement brings the neural precursors to the dorsal midline to form the neural keel (Gibson, 2014). The neural keel eventually develops a lumen and is internalized to become the neural tube (Gibson, 2014). The end result of involution at the margins is the three major germ layers: the

ectoderm, mesoderm, and endoderm.

The regional (dorsal, ventral, anterior, posterior) identity of tissues in the embryo is controlled by growth factors, paracrine factors, transcription factors, and all of the genes activated by the primary signaling molecules. Expression of bone morphogenetic protein (BMP) and wingless/int-1 (Wnt) induce ectodermal tissues to become epidermis. Zebrafish, specifically, express BMP2B to cause cells to take on ventral and lateral fates. Wnt8b induces embryonic tissues to have ventral, lateral, and posterior fates (Gibson, 2014). In order for neural tissues to form on the dorsal side of the embryo BMP2B and Wnt8 must be inhibited. Inhibition of BMP2B is accomplished through translation of maternally deposited β-catenin transcripts in the endodermal cells in an area just below the dorsal shield (Gibson, 2014). β-catenin is stabilized in concert with Wnt signaling in the dorsal shield and will interact with Tcf3 to form a transcription factor that activates genes with dorsalizing capabilities like *FGF*, *Squint*, and *Bozozok* (Gibson, 2014). Many of these genes act directly to inhibit repressors such as BMPs and Wnts, and also activate neural genes like *goosecoid*, *noggin*, and *dickkopf* (Gibson, 2014).

The Wnt ligand and its receptor, Frizzled-low density lipoprotein receptor related protein (Fz-LRP) both have multiple isoforms. The way in which the combinations of these isoforms affects eye field specification has not been fully resolved. This is due largely to the fact that Wnt and Fz-LRP can also signal non-canonically, independent of the β-catenin pathway (Sernagor 2006). In zebrafish for example, Wnt8b and Fz8, signal within the canonical β-catenin pathway and inhibit eye field formation (Sernagor 2006). Conversely, Wnt11 and Fz5 promote eye field specification through non-canonical

antagonism of the Wnt β-catenin pathway (Cavodeassi, Carreira-Barbosa et al. 2005). Recent research supports a model in which there is a balance between canonical and non-canonical Wnt/Fz-LRP signaling that promotes eye field specification (Fuhrmann 2008; Sernagor 2006).

Similarly, neural ectoderm is patterned in an anterior posterior manner by the combination of different levels of retinoic acid (RA), FGFs and Wnts. RA at high levels induces cells to take on a posterior fate while low levels of RA allows for cells to develop an anterior identity (Gibson, 2014). Low levels of RA are achieved by the expression of the *cyp26* gene, encoding retinoic acid-4-hydroxylase which will break down RA (Gibson, 2014).

Neural induction, brain segment specification, eye field specification, and eventually development of the eye are dependent upon a series of transcription factors (Zuber, Gestri et al. 2003). Noggin and other neural inducers help to specify the neural plate (Figure 1.2.0). Noggin activates Otx2, specifying the forebrain and midbrain. ET and Rx1sequentially activate, leading to Pax6 and Six3 activation (Zuber, Gestri et al. 2003) (Figure 1.2.0). The rest of the network comes online, including tII and Lhx2 followed by Optx2 later in development (Zuber, Gestri et al. 2003) (Figure 1.2.0). These gene activations cause the optic vesicle to evaginate from the forebrain via the optic stalk (Chang and Min 2011). The lens placode is formed in the surface ectoderm. When the optic vesicle comes into contact with the lens placode, just before 20 hpf, extension completes, and the vesicle is formed into the optic cup (Chang and Min 2011). The ventral optic fissure, which allows blood vessels to pass to the mesenchyme, forms

ventrally at 24 hpf and closes by 48 hpf (Chang and Min 2011). Neurogenesis begins near 28 hpf and the optic fissure then closes at 48 hpf. The visual system is largely complete and has baseline function at 72 hpf (Chang and Min 2011).

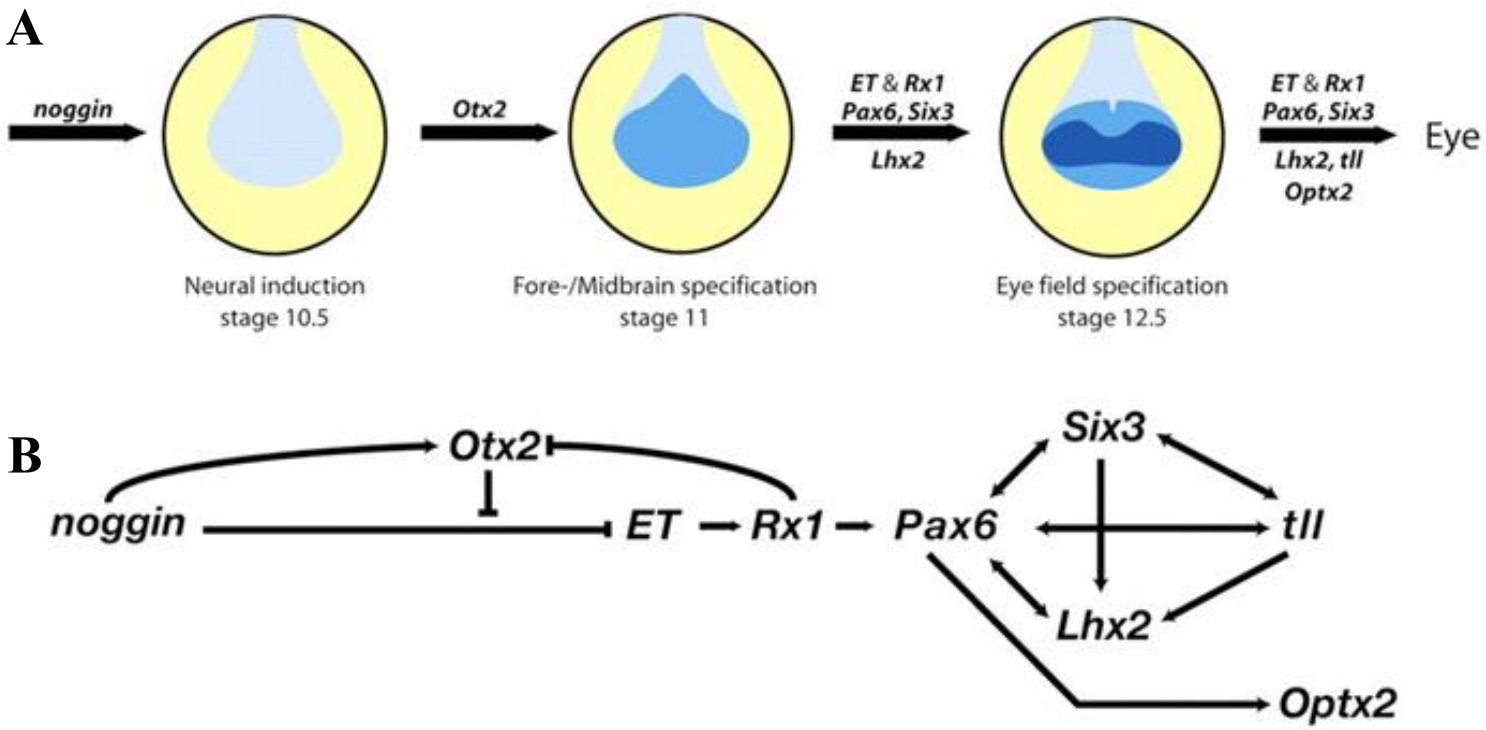

Figure 1.2.0. Progression of eye development in vertebrates. Neurogenesis from neural induction to eye development and the genes required for each successive stage (A). Early transcription factor network (EFTF) interactions necessary for proper eye development (B). Adapted from Zuber, Gestri et al. 2003. Permissions granted by Company of Biologists, license number: 3597210552546.

Retinal Differentiation

The retina is a complex nervous tissue that evolved to accept photo information from the surrounding environment and relay it to the brain. The retina has a laminated structure, with each layer contributing to the overall function of the system (Figure 1.2.1 B). The retinal pigmented epithelium (RPE) is the outermost layer of the retina and lies between the photoreceptors and the choroid, the vascular layer of the eye (Strauss, 1995). As the outermost layer of the retina and the retina/blood barrier, the RPE is critical for absorbing light, maintaining the photoreceptor population, controlling ion homeostasis in the retina, and moving unwanted water and metabolites out of the retinal space (Strauss, 1995). Rod and cone photoreceptors in the outer nuclear layer (ONL) are able to convert light into chemical and electrical signals that can be passed onto bipolar inter-neurons in the outer plexiform layer (OPL) (Sernagor, 2006).Transmission of the signal from the ONL to the inner nuclear layer (INL) is also supported by the horizontal interneurons which are in contact with bipolar neurons. Bipolar interneurons synapse with retinal ganglion cells (RGCs) and amacrine interneurons in the inner plexiform layer (IPL) (Sernagor, 2006). Amacrine cells modulate the signal coming from the bipolar interneurons by inhibiting the RGCs directly and also inhibiting transmitter release from the bipolar neurons (Sernagor, 2006). RGCs then pass the signal through their projections, the optic nerve or tract, to the optic tectum; which is the visual interpretation center of the brain.

Each neuron type in the retina has critical and specific function that is intimately tied to its position. For this reason retinal differentiation must occur in an organized

manner for the proper cell types to be born in their respective layer and correct synapses to form. RPCs in the early optic vesicle and cup migrate along processes that extend to the basal and apical sides of the nueroepithelium, in a process known as interkinetic nuclear migration (Figure 1.2.1 A).

The mechanisms that regulate interkinetic nuclear migration within the retina have not been comprehensively described. However, investigations of nervous tissue development in other areas of the nervous system have shown that Cdk5 and focal adhesion kinase signaling are critical to the process (Sernagor 2006). Naturally, somal translocation also involves the cytoskeleton and micro-tubule based motors that will actually move the nucleus through the cell (Sernagor 2006). During G1, progenitors migrate towards the basal surface of the neuroepithelium. S-phase take place near to the basal surface and G2 begins as progenitors move back towards the apical surface. M-phase occurs when the RPCs reach the apical surface. Apical surface division means early born cells that reside near the central retina have much further to migrate. The inner and outer layers of the zebrafish retina are formed first, with the RGCs and cones being first to differentiate. However, birth of different neuron types is not sequential with regard to position and multiple neuron types may be differentiating simultaneously (Figure 1.2.1 B and C). During M-phase RPCs retract processes and then divide in two fashions. Symmetrical division results in two undifferentiated daughter cells and asymmetrical division gives rise to one undifferentiated daughter and one daughter that will migrate and differentiate (Sernagor, 2006). During the first 16 hpf, RPCs undergo a number of rapid symmetrical divisions, bolstering the population of RPCs. Cell cycle

times during this stage are 8 to 10 hours. From 16 to 24 hpf, cell cycle times reduce considerably, dropping to 32-49 hrs, and asymmetric division begins to occur resulting in the birth of the first neurons (Sernagor, 2006). The physiological function of the drop in cell cycle time is not well-characterized, although it is thought that the longer cell cycle times allow for growth of the retina to accommodate new cell types being born. Another rationale suggests the RPCs revert to symmetrical division to repopulate the RPC pool before the next neuronal subtype is differentiated (Sernagor, 2006).

The differentiation of neuron types during retinal histogenesis follows a tight developmental timeline. Cells differentiating in the retina are influenced by a multitude of factors in the extracellular environment including feedback inhibition by differentiated cells, extracellular signals such as sonic hedgehog (shh), and the intrinsic constituents of the cell itself. The combinatorial effect of these extracellular cues has not been completely characterized. However, the activation of the proneural basic helix-loop-helix transcription factors in response to the full suite of signals is better known. The combination of bHLH transcription factors being expressed at a given time coincides with birth of the different neuron types (Figure 1.2.1 C). 28 hpf RGCs differentiate in a wave from the central retina in response to a signal from Shh, and activation of transcription factors Atonal and Neurog (Fadool and Dowling, 2008) (Figure 1.2.1 C). Differentiation of amacrine cells and interneurons occurs shortly thereafter, and under the expression of Atonal, Neurog and Neurod (Fadool and Dowling, 2008) (Figure 1.2.1 C). By 48 hpf, Muller glia, bipolar cells, and rods begin to differentiate under expression of Neurog, Neurod, and Ascl (Fadool and Dowling, 2008) (Figure 1.2.1 C). By 72 hours, all

the cells of the retina are present and baseline visual function is established. It is clear from the expression of multiple bHLH genes at a given time that determination of cell type is dictated by the combinatorial effect of the transcription factors activated, soluble signals in the retinal environment, and other extracellular cues.

Once the structures of the eye are complete and visual function is established, the eye will continue to grow in size. Maintenance of the eye also becomes important as the fish progresses into adulthood. Expansion of the eye toward the end of development and maintenance of cells during the lifetime of the fish relies on the ciliary or marginal zone on the periphery of the retina. Stem cells residing in this location provide the eye with the cells necessary to increase eye size in the latter stages of development and replenish lost cells throughout the fish's lifetime (Sernagor 2006).

Development of nervous tissues is a highly organized process and requires proper temporal and spatial control. For this reason, many processes in nervous tissue development, like interkinetic nuclear migration, are highly conserved in different nervous tissues. While CrkL was the link between DCBLD2 and nervous tissue development and had only been implicated in brain development, conservation of developmental processes gave us confidence in using the zebrafish eye to explore dcbld2 function in nervous tissue. Based on previous research and the newly found association of DCBLD2 and the CrkL-SH2 domain, we hypothesized that dcbld2 plays a role in the developing nervous tissue of the zebrafish eye. We aimed to test if dcbld2 was expressed in the zebrafish, and if so, where it was localized. Another goal of the thesis was to test

what affects dcbld2 receptor knockdown would have on the developing nervous tissue.

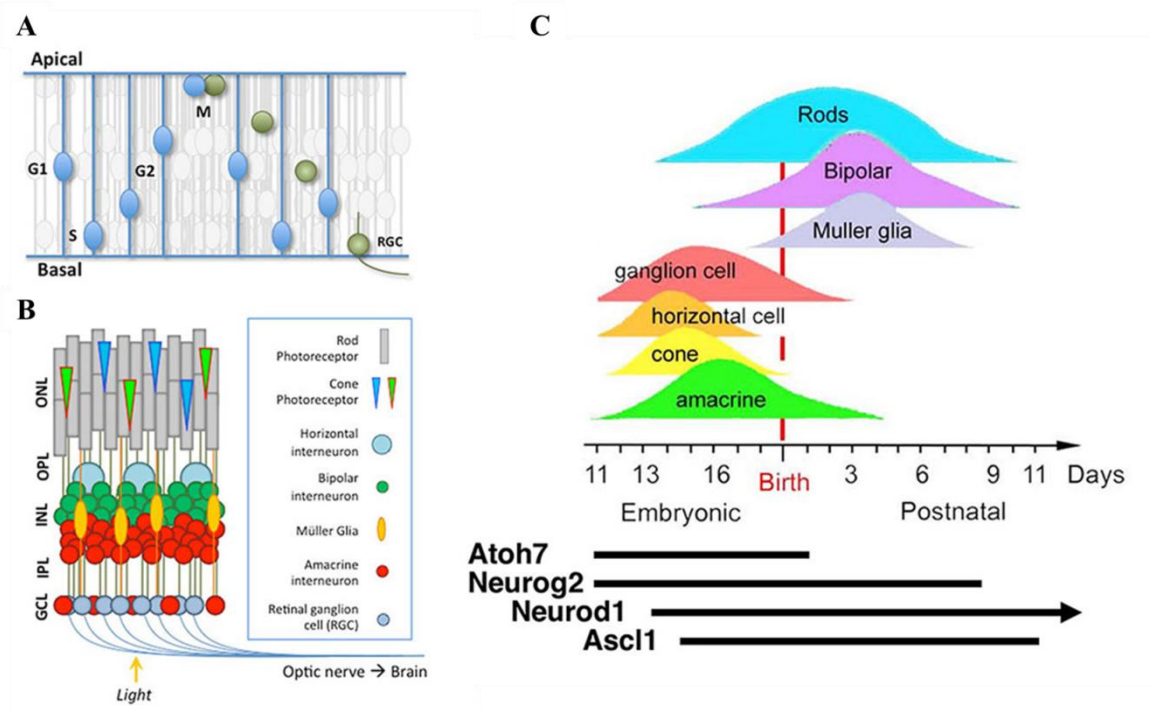

Figure 1.2.1. Interkinetic nuclear migration and retinal differentiation. Retinal precursors migrate from the apical to basal surface while progressing through the cell cycle (A). The complete retina is a highly organized laminated structure with neurons in the nuclear layers passing information via synapses in the plexifom layers (B). Different neuron populations are generated at different times of development and can be linked to the expression of certain bHLH transcription factors (C). Reproduced from Hufnagel and Brown, 2013, and with Permission from N.L. Brown (Figure C, unpublished).

MATERIALS AND METHODS

In Situ Probe Creation

Amplification of *dcbld2* was performed from isolated zebrafish cDNA and cloned into the pCRII-TOPO vector (Invitrogen) using BamH1 and NotI restriction sites. PCR primers used in amplification of the *dcbld2* for probe creation are listed below.

Forward primer: 5'- ACCGCTTCAAGAGTTCAGGA -3'
Reverse primer: 5'- TTGTGGTGTGGTCCACTCAT-3'

The template for probe creation was made from 1 µg of linearized pCRII-TOPO-*dcbld2* vector. To create the probe, 1 ug of *dcbld2* transcript template was mixed with 10 µl of 20 mM dithioreitol, 4 ul of transcription buffer (Promega), 2 µl of DIG RNA labeling mix (Roche), 1 ul of 2mg/ml of RNAse inhibitor (Invitrogen), 1 µl (20 units) of SP6 (Promega) or T7 polymerase (Affymetrix), and the reaction was brought to a total volume of 20 µl with nuclease free water. The reaction was incubated for 3 hours at 37ºC before 1 µl (2 units) of DNAse (Ambion) was added. Following incubation, 2 µl of .5 M ethylenediaminetetraacetic acid (EDTA), 2.5 µl of 500 mM lithium chloride (LiCl), and 100 µl of 100% EToH were added for a final volume of 124.5 µl. RNA was precipitated overnight at -20 ºC. RNA was spun down (Eppendorf 5415C), washed with 70% EtOH, and then resuspended in 20 uL of water. The RNA probe was then added to hybridization buffer comprised of 50% formamide, 5X SSC, 0.1% Tween-20, and 5mg/ml tRNA, and maintained at -20 ºC in separate aliquots.

In Situ Probe Hybridization

Dechorionated embryos at a range of developmental stages were fixed in 4% paraformaldehyde (PFA) in phosphate buffered saline (PBS). Embryo's for *in situ* hybridization were dehydrated in 100% methanol (MeOH) then stored in 100% MeOH at -20 ºC. Embryos were rehydrated in successive 5 minute washes: 100% MeOH, 75% MeOH and 25% PBS, 50% MeOH and 50% PBS, 25% MeOH and 75% PBS, and then washed 3 times in 100% phosphate buffered tris (PBT). Embryos were then permeated with 10 mg/ml of proteinase K (Promega) (24 hpf: 0 min, 48 hpf: 15 min, 72hpf: 30 min), and washed 3 times in 100% PBS. The anti-sense or sense probe was then added to additional hybridization buffer in 1:100 ratio, placed onto embryos, and stored overnight at 70 ºC. 15 minute successive washes of hybridization buffer and saline-sodium citrate (SSC) equilibrated the embryos; 100% hybridization buffer, 75% hybridization buffer and 25% 2X SSC, 50% hybridization buffer and 50% 2X SSC, 25% hybridization buffer and 75% 2X SSC, and then 2X washes of 2X SSC for 30 minutes. Embryos were then washed twice for 30 minutes in 0.2X SSC. Rehydration was completed with 10 minutes successive washes of 0.2X SSC and PBT: 100% 0.2X SSC, 75% 0.2X SSC and 25% PBT, 50% 0.2X SSC and 50% PBT, 25% 0.2X SSC and 75% PBT, and 100% PBT.

Anti-digoxigenin-AP (Roche - 11093274910) diluted 1:5000 in *in situ* block (PBS, 5% normal sheep serum, and 1% bovine serum albumin) was added to embryos and incubated at room temperature for 2 hours. Anti-digoxigenin solution was removed and embryos were washed 3 times for 10 minutes in PBT. Nitro-blue tetrazolium chloride and 5-bromo-4-chloro-3'-indolyphosphate p-toludine salt (NBT/BCIP; Thermo

Scientific) were added to embryos incubated with anti-sense or sense probes and incubated until staining had reached desired contrast. Side by side sense control probe staining was completed to ensure binding was specific. 4% PFA was added to halt staining reaction and embryos were stored in PBT at 4℃ for further processing.

Morpholino Injection and Embryo Care

Fertilized embryos were collected at the 1 cell stage and injections were completed on an Eppendorf FemtoJet microinjection system. A Nikon SMZ800 dissecting scope was used to inject a 4 unit bolus at 3.2X magnification. A pressure of 80-100 PSI was normally sufficient to inject the proper amount of solution. 0.1% rhodamine was co-injected as a loading control. Embryos were collected and stored in egg water (0.6 g/L aquarium salt, 0.01 mg/L methylene blue) at 28.5 ºC. At 24 hours, phenylthiourea was added to egg water to a final concentration of 0.003% to prevent pigment generation as previously described (Karlsson, von Hofsten et al. 2001).

A *dcbld2* splice site (intron 1, exon 2) blocking morpholino (Gene Tools LLC), as previously described (O'Connor, Salles et al. 2009), was employed to knockdown the receptor (Figure 1.4.1 C). Morpholino was diluted down to 500 µM for injections. 6 , 5 , 3, and 1 ng morpholino injections were conducted to evaluate broad effect and toxicity of the morpholino. Morpholino sequence is listed below.

DBCLD2 SP1 Morpholino – AGCCGTCCCCTGAAAAACACCCAGA

Morpholino Knockdown Verification

50 morphant or un-injected control (UIC) embryos (48hpf) were collected and added to 100 µl of trizol (Invitrogen). The embryos were incubated overnight at -20 ºC. Embryos were homogenized and an additional 900 µl of trizol (Invitrogen) was added. The homogenate was incubated at room temperature for 5 minutes. 200 µl of chloroform (Fisher) was added and the homogenate was vortexed for 15 seconds and then incubated for 5 minutes at room temperature. The homogenate was then spun (Eppendorf 5415C) at 12,000 rpm for 5 minutes in a 4 ºC cold room. Trizol and chloroform cause a phase separation and will cause the RNA to become isolated in the aqueous layer. The aqueous layer is extracted, added to 500 µl of isopropyl alcohol, incubated for 5 minutes at room temperature, spun (Eppendorf 5415C) for 5 minutes at 12,000 rpm at 4 ºC, and the isoporopyl alcohol was removed from the tube. 1 ml of 75% EtOH is used to wash the RNA by spinning for 5 minutes at 4 ºC. The EtOH was removed and RNA dried at room termperature. The RNA was then resuspended in 50 µl of nuclease free water. RNA concentrations were measured with a nano-drop (Thermo Scientific) to allow for synthesis of both UIC and MORPHANT cDNA from the same quantity of RNA. cDNA was synthesized as previously desrcribed (Peterson and Freeman 2009), and run out on an agarose gel to determine transcript levels of EF1α and DBCLD2 in UICs, 5 ng (400 µM) injected morphants, and 3 ng (250 µM) morphants.

RT-PCR morpholino verification primers to ensure knockdown of the protein were designed against zebrafish *dcbld2* and used in tandem with housekeeping gene EF1α primers as a control and for normalization. The PCR program for morpholino

verification is listed below:

PCR Program (30 cycles): 2 minutes at 95 ºC; 30 seconds at 95 ºC; 30 seconds at 50 ºC; 45 seconds at 72 ºC; 5 minutes at 72 ºC. Hold at 4ºC.

5 ng (400 mM) and 3 ng (250 mM) ng injection quantities were characterized more fully with densitometry (Figure 1.4.1 C), and H&E stained sections (Figure 1.4.1 B). A P53 morpholino , as previously described (Robu, Larson et al. 2007), was injected at 1.5X quantity (4.5 ng or 375 mM) with the 3 ng 2 morpholino dose. The P53 morpholino sequence is listed below.

P53 Anti-sense Morpholino: 5'- GCGCCATTGCTTTGCAAGAATTG -3'

The P53 morpholino blocks the cell death cascade and can demonstrate specificity of the target morpholino being used by controlling for off-target cell death (Figure 1.4.1 A and B). Retinal diameters were also measured to ensure similar nervous tissue generation in the P53 and dcbld2 co-injections, and dcbld2 injections alone (Figure 1.4.1 F). After evaluation of the morpholino effect, a 3 ng injection quantity was selected for use in the subsequent experiments.

Assessing Optic Tract Formation

The *Isl2b:GFP* transgenic line, as previously described (Pittman, Law et al. 2008), was used to assess optic tract development as a product of RGC differentiation and axon extension (Figure 1.4.3 A). Embryos were anesthetized with a solution of .2 g Tricaine (Western Chemical Inc.), 0.5 g Na_2HPO_4, and 50 ml 1X egg water in petri

dishes. Tracts were scored on a normal, weak, or absent basis (Figure 1.4.3 A). UIC and morphant embryos that had no GFP expression were not counted in scoring and only embryos that showed GFP expression in other structures (cranial ganglia), but not in optic tracts were counted as absent. In order to quantify differences, "weak" and "absent" embryos were binned together. Quantitative comparisons were then carried out between UICs and morphants based on the percent of normal optic tracts each group had at 48 hpf and 72 hpf (Figure 1.4.3 C).

Imaging and Eye Measurements

Optic tract scoring was completed on a Olympus IX71 inverted fluorescence microscope in real time. The IX71 was fitted with a SPOT Insight™ 4 digital camera to image zebrafish eye sections (H+E, DAPI) at 20X magnification. Exposure and brightness was controlled automatically by SPOT Basic Image Capture software.

A Nikon SMZ800 dissecting microscope equipped with a SPOT Insight™ 4 digital camera was used to take whole mount images. SPOT Basic Image software was used to make measurements of retinal diameter, eye area, and lens area. Calibration of software was set to image specifications before measurements were conducted. Scale bars on all eye images represent 50 µm.

Confocal imaging was completed on a Nikon Eclipse T*i* microscope with Nikon C2S*i* software. Embryos were positioned in 1% low melt agarose and 5 µm stepwise sequential images (Z stack) were taken. Z stacks were flattened into a single max brightness image and were cropped in Adobe Photoshop

Embedding, Sectioning and Staining

Embryos to be embedded were fixed in 4% PFA. To allow for perfusion of polymerizing resin, embryos were dehydrated in 100% EtOH overnight at 4 ºC, and then infiltrated with the monomer of the embedding substrate (reagents A&C; Polysciences INC) for 1.5 hours at room temperature, before adding the polymerizing catalyst (reagent B; Polysciences Inc). Embryos were then positioned and casted in JB-4 (Polysciences Inc) resin as previously described (Sullivan-Brown, Bisher et al. 2011).

A Leica RM2265 microtome was used for all sectioning. Zebrafish were sectioned in a transverse plane across the front of the head an eyes. All sections were cut at a thickness of 7 µm, water floated, and heat adhered to Super Frost (Fisher) microscope slides.

For RGC counts embryo sections were DAPI stained and coverslipped. VECTASHIELD hardmount mouting medium was applied to slides, coverslipped, and allowed to set for 3-4 hours. Images of central retina sections were captured and cells in the RGC layer were counted using Image J software. Displaced amacrine cells often reside in this layer during development, and so it is not appropriate to refer to the cells as RGCs alone.

Sections were rehydrated in water for 5 minutes. Sections were stained in 6.0% hematoxylin, 0.2% aluminum ammonium sulfate dodecahydrate, 0.2% methanol, and 4.8% methanol for 9 minutes. Washed in water twice for 5 minutes, and then stained with eosin (solution) for 45 seconds. Slides underwent 3 final washes at 2 minutes each before

being viewed and imaged.

Zebrafish Use and Care

All work involving zebrafish was authorized by the University of Vermont Institutional Animal Care and Use Committee (Protocol #12-055). Zebrafish were kept on a 14 hour light, 10 hour dark cycle. Zebrafish were maintained and bred as described previously (Brand, Granato et al. 2002).

Statistical Analysis

All measurements were converted and exported from SPOT Basic Image Capture software to GraphPad Prism (V 6.0). All comparisons were made with an unpaired Students t-test assuming equal variance. Error bars represent standard error of the means on all graphs. For results to be deemed significant a cutoff of $P<0.05$ was used. Indicators of significance level are as follows; ****: $P<0.0001$, ***: $P<0.001$, **: $P<0.01$, and *: $P<0.05$.

RESULTS

In Situ Hybridization

To determine where *dcbld*2 mRNA was expressed in the developing zebrafish embryo, *in situ* hybridizations with a dcbld2 anti-sense and sense mRNA probe were conducted. The anti-sense probe will bind where dcbld2 transcript harboring the reverse compliment to the probe is being expressed and the sense probe is used as a negative control to evaluate the level of non-specific binding under the same staining procedures. Staining is only indicative of transcript expression and while it guides further study, does not directly indicate protein presence in that location. 24, 48, and 72 hpf embryos were evaluated for the *dcbld*2 expression.

At 24 hpf the anti-sense probe bound strongly in the head and eye region (Figure 1.4.0). While the staining shows expression throughout the head and eye, localization is specific to areas of nervous tissue development. The developing eye field has staining, as do the presumptive regions of the developing prosencephalon, mesencepahalon, and notochord (Figure 1.4.0 B and E). The lateral view shows apparent staining in the midbrain hindbrain boundary, where the cerebellum will form (Figure 1.4.0 B). Dorsal view of the 24 hpf embryo highlights staining within the developing eye fields and in the midline of the embryo (Figure 1.4.0 E). The sense control probe, displayed at 24 hpf, showed markedly lower signal at all time points (Figure 1.4.0 A).

48 hpf embryos had expression of the *dcbld2* transcript in the same areas as the 24 hpf embryo, but also showed a more ubiquitous expression pattern. The head and the eye

still have strong transcript expression, but it is difficult to discern individual structures from the lateral view at this time point (Figure 1.4.0 C). The dorsal image shows expression more specifically contained within the regions of the developing brain including the myelencephalon, mesencephalon and diencephalon (Figure 1.4.0 F). The staining extending past the developing brain regions is diffuse and dissipates posteriorly, but was not considered non-specific.

The 72 hpf embryos again showed specific staining in the head and eye regions. Transcript localization of dcbld2 included the telencephalon, tectum and retina. Staining is lighter, but it also appears to be present in the cerebellum (Figure 1.4.0 D and G). The dorsal view shows clear staining in the eye, specifically the regions of the retina surrounding the lens, and the same brain regions as in the 48 hpf embryo (Figure 1.4.0 G).

In situ hybridization of the dcbld2 probe shows the mRNA of the protein being expressed in developing nervous tissue, including the brain and eye regions. Staining beyond the nervous tissue is most likely attributed to *dcbld2* being expressed in the vasculature and or patterning of smooth muscle involved in these systems (Sadeghi, Esmailzadeh et al. 2007). However, there is currently no *in situ* hybridization data available for dcbld2, making it necessary to rely on the consistency of repeated trials. mRNA expression patterns were consistent over 4 different *in situ* hybridization experiments. It is possible that *dcbld2* expression in non-neuronal tissues is contributing to the staining observed, but nervous tissue will remain the focus of this work. Function of dcbld2 in nervous tissue, at least in the retina, will be addressed in more detail in the

following sections.

The timeline for *dcbld2* expression roughly matched the window of retinal neurogenesis. The first neurons in the eye turn on around 28 hpf (RGCs), and by 72 hpf the eye is still growing but mostly complete. At 24 hpf the receptor is expressed in areas of neuronal development, the presumptive brain regions and eye, but it is rather diffuse and only seems to have specific localization in the cerebellum. At 48 hpf, a time at which nervous tissue is differentiating, the staining strengthens in the head and eye but is also more widespread through the embryo (Figure 1.4.0 C). However, the staining is also more localized within specific structures in the head and eye region. Both the developing brain regions and the eye have mRNA expression of *dcbld2* that is higher than surrounding tissues (Figure 1.4.0 C and F). Overall, it is clear that *dcbld2* is expressed in nervous tissue and at time points that match nervous tissue development. This data was consistent with our proposed functions for dcbld22 and allowed for the progression of the project to more fully characterize DCBLD2 function in zebrafish.

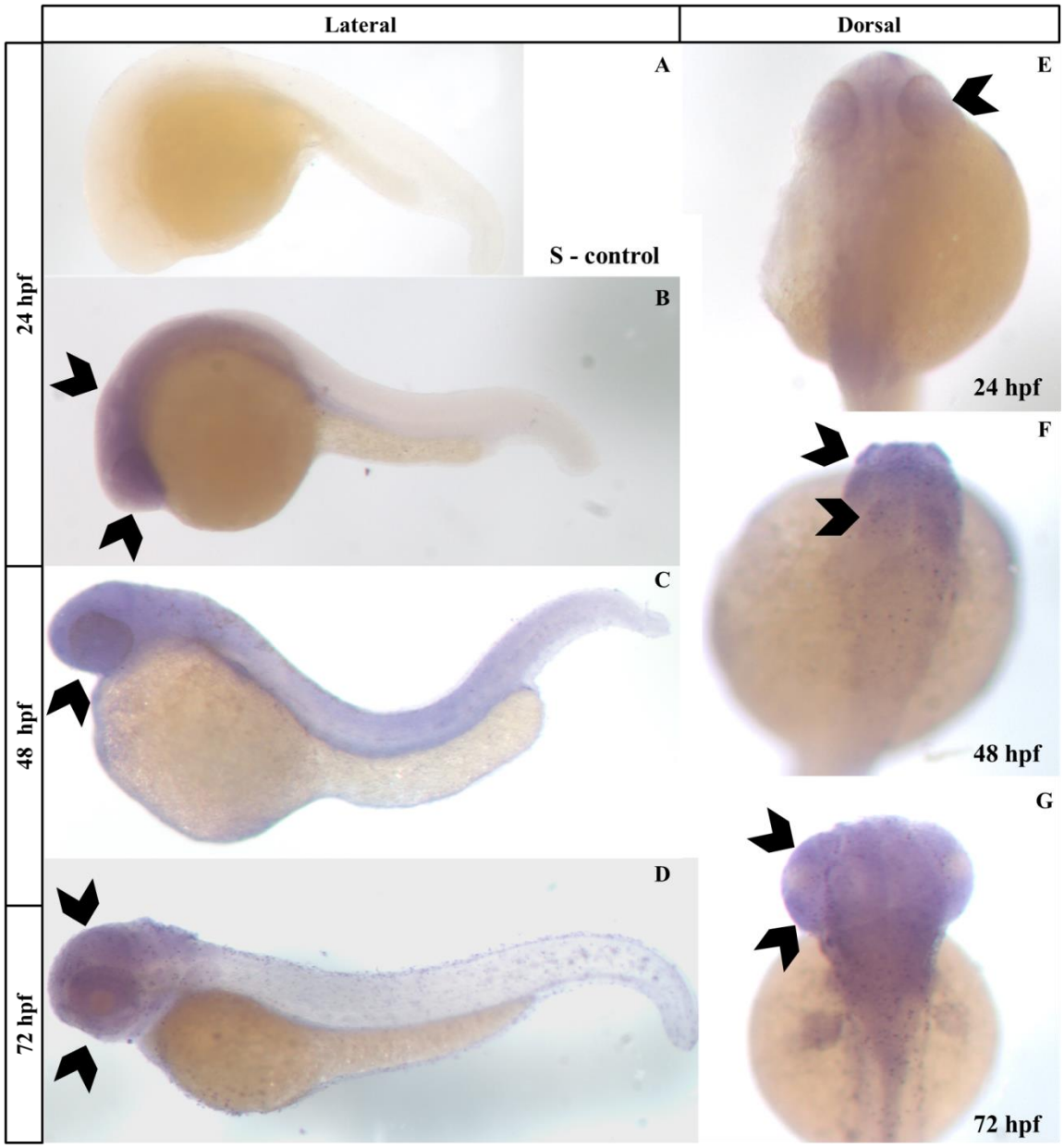

Figure 1.4.0. dcbld2 mRNA is expressed in developing nervous tissues. The sense probe negative control at 24 hpf shows negligent non-specific binding, which was true of the 48 and 72 hpf embryos as well (A). dcbld2 is expressed in the head and eye (arrows) at 24 hpf, including regions of prosencephalon, mesencephalon, and notochord development (B, E). 48 hpf embryo showed slightly more global expression, but similar expression in the developing eye and brain regions (arrows). At 72 hpf dcbld2 is restricted to the head region only, being expressed strongly in the telenchaphalon, tectum, and the retinal region surrounding the lens (D, G, arrows: eye and brain).

Morpholino Protein Knockdown

Knockdown of dcbld2 by morpholino resulted in developmental defects of the eye, including a loss of lamination. After observing a phenotype, a morpholino dose response experiment was carried out to gauge the penetrance at specific dosages, to gauge how much of the total message was knocked down, and to distinguish a suitable injection amount to knockdown the receptor without causing toxicity.

To assess knockdown efficiency *dcbld2* was amplified by RT-PCR from 48 hpf fish homogenates and normalized to the housekeeping gene elongation factor 1 alpha (EF1α) (Figure 1.4.1 D and E). 48 hpf embryos were selected for morpholino validation because they would still be within the period of retinal neurogenesis and the time point makes conducting multiple experiments feasible.

5 ng of morpholino was sufficient to almost completely ablate transcript synthesis, but was embryonic lethal and resulted in a grossly malformed embryo (Figure 1.4.1 A, B, D, and E). A 3ng injection knocked down the transcript down close to 50% , the loss of lamination phenotype was still present and the embryos were able to survive (Figure 1.4.1 A, B, D, and E). The 3ng morpholino dose still had a visible effect on embryos, but the morphants underwent a mostly normal development; all of the major structures developed and the embryos survived well past early development (Figure 1.4.1 A).

To examine if the dcbld2 morpholino initiated non-specific cell death-based effects, a P53 morpholino was co-injected to inhibit off-target cell death. The P53 protein

mediates the cell death cascade that is potentially activated in response to toxicity caused by high levels of morpholino (Robu, Larson et al. 2007). By simultaneously injecting a P53 morpholino with the target morpholino, it is possible to inhibit off-target cell death and determine if non-specific cell death is contributing to a phenotype. The co-injection of P53 morpholino with 3ng of dcbld2 morpholino indicated that off-target cell death was not a major contributor to the phenotype (Figure 1.4.1 A and B). However, due to an apparent loss of nervous tissue in the morphant without the P53 morpholino, eye diameters were measured to ensure the phenotype in the eye was specific (Figure 1.4.1 F). The UIC retinal diameters (n = 32) were statistically different than both the morphants (n = 35) and P53 co-injected embryos (n = 8) ($P<0.0001$, unpaired Student's t-test). The dcbld2 morphants and P53 co-injected embryos did not show a significant difference between each other in their retinal diameters ($P>0.05$, unpaired Student's t-test).

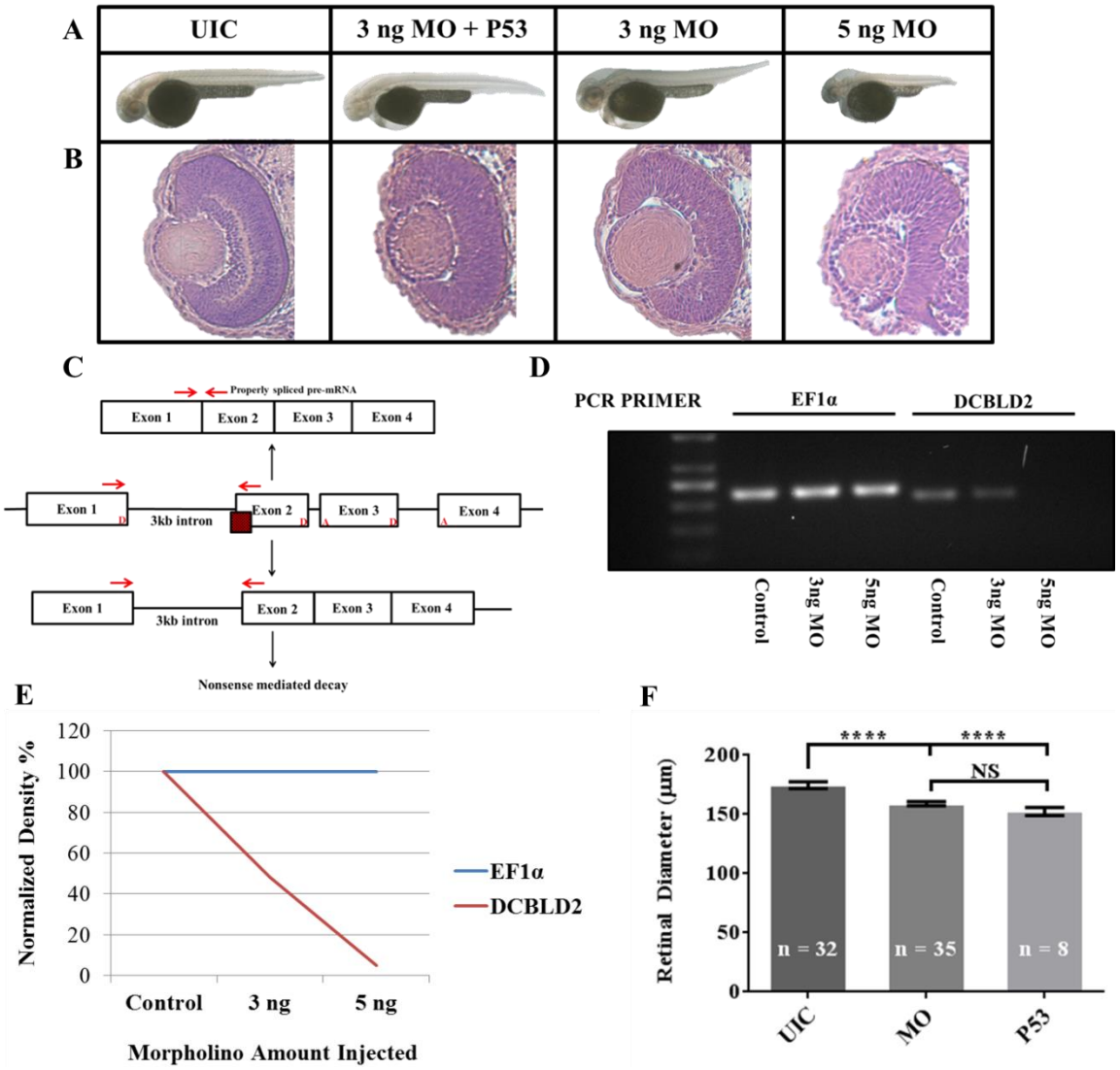

Figure 1.4.1. Morpholino dose response in 48 hpf zebrafish. Whole mount and central retinal sections of UIC, P53 and dcbld2 coinjections, 3 ng morphants, and 5 ng morphants (A, B). dcbld2 splice site morpholino results in the erroneous inclusion of intron 1 an aberrant protein product that would likely be removed via nonsense-mediated decay (C). 3 ng morpholino injections resulted in the observed lamination phenotype, caused minimal off-target effects, and knocked the receptor down to 52% when normalized to EF1α (A, B, D, E). Retinal diameter measurements were consistent with P53 co-injections, showing that the UIC differed from both the morphants and co-injected embryos, but the morphants were not significantly different from the co-injected embryos (F, ****P<0.0001, NS = P>0.05, unpaired Student's t-test).

dcbld2 Knockdown Affects RGC Differentiation and Optic Tract Formation

Injection of the dcbld2 morpholino into the *Isl2b:GFP* transgenic line enabled us to evaluate RGC differentiation throughout development, including optic tract formation. The *Isl2b:GFP* transgenic confers green fluorescence to RGCs, rohon-beard neurons, and cranial-ganlgia. The UIC and dcbld2 morphants did not show distinct changes in overall morphology, although we had noticed that morphant eyes were often smaller (Figure 1.4.2 A and B). However, dcbld2 morphants clearly had less RGCs differentiating by 48 hpf, with a good portion of the clutch showing no differentiation at all (Figure 1.4.2 C and D). By 72 hpf most morphant fish had some differentiation of RGCs occurring, but still lacked in overall RGC populations compared to UIC (Figure 1.4.2 E and F). Cranial ganglia in both the morphants and UIC seemed to develop normally and showed strong fluorescent signals, suggesting the promoter for the GFP was working properly.

To evaluate these differences, optic tracts were scored on a normal, weak, or absent scale (Figure 1.4.3 A). UIC and morphant embryos that had no GFP expression were not counted in scoring and only embryos that showed GFP expression in other structures (cranial ganglia), but not in optic tracts, were counted as absent. 77% of 48 hpf UICs (n = 696) had normal optic tracts, 14% had weak, and 9% had no optic tracts (Figure 1.4.3 B). This contrasted to the 48 hpf morphants (n = 1754) where 25% had normal optic tracts, 45% had weak, and 30% were completely deficient in optic tracts (Figure 1.4.3 B). By 72 hpf we did see the morphants recovering somewhat, but they never reached UIC levels of differentiated RGC. 94% of UICs at 72hpf (n = 451) had normal optic tracts, 5% had weak optic tracts, and 1% with no optic tracts forming

(Figure 1.4.3 B). Morphant embryos (n = 1216) at 72 hpf had only 40% of fish with normal optic tracts, 46% with weak optic tracts, and 14% with no optic tracts (Figure 1.4.3 B).

To compare these groups statistically, absent and weak optic tract classifications were binned together and compared against the normal. The percent of normal optic tract development was then plotted (Figure 1.4.3 C). 10 experiments with at least 15 embryos per experiment were included in the analysis. UIC and morphants were significantly different at 48 hpf, with 75% of UICs having normal optic tracts and only 25% of morphants having normal optic tracts (Figure 1.4.3 C, $P<0.0001$, unpaired Student's t-test). This result was consistent with the comparison at 72 hpf, when UICs had normal optic tracts 94% of the time and morphants only 40% of the time (Figure 1.4.3 C, $P<0.0001$, unpaired Student's t-test). Importantly, when UICs at 48 hpf are compared to morphants at 72 hpf, the UIC still have a greater proportion of fish with normal optic tracts (Figure 1.4.3 C, $P<0.0001$, unpaired Student's t-test). While morphant fish do have some late RGCs differentiating they cannot overcome the effects from loss of the dcbld2 receptor early in development.

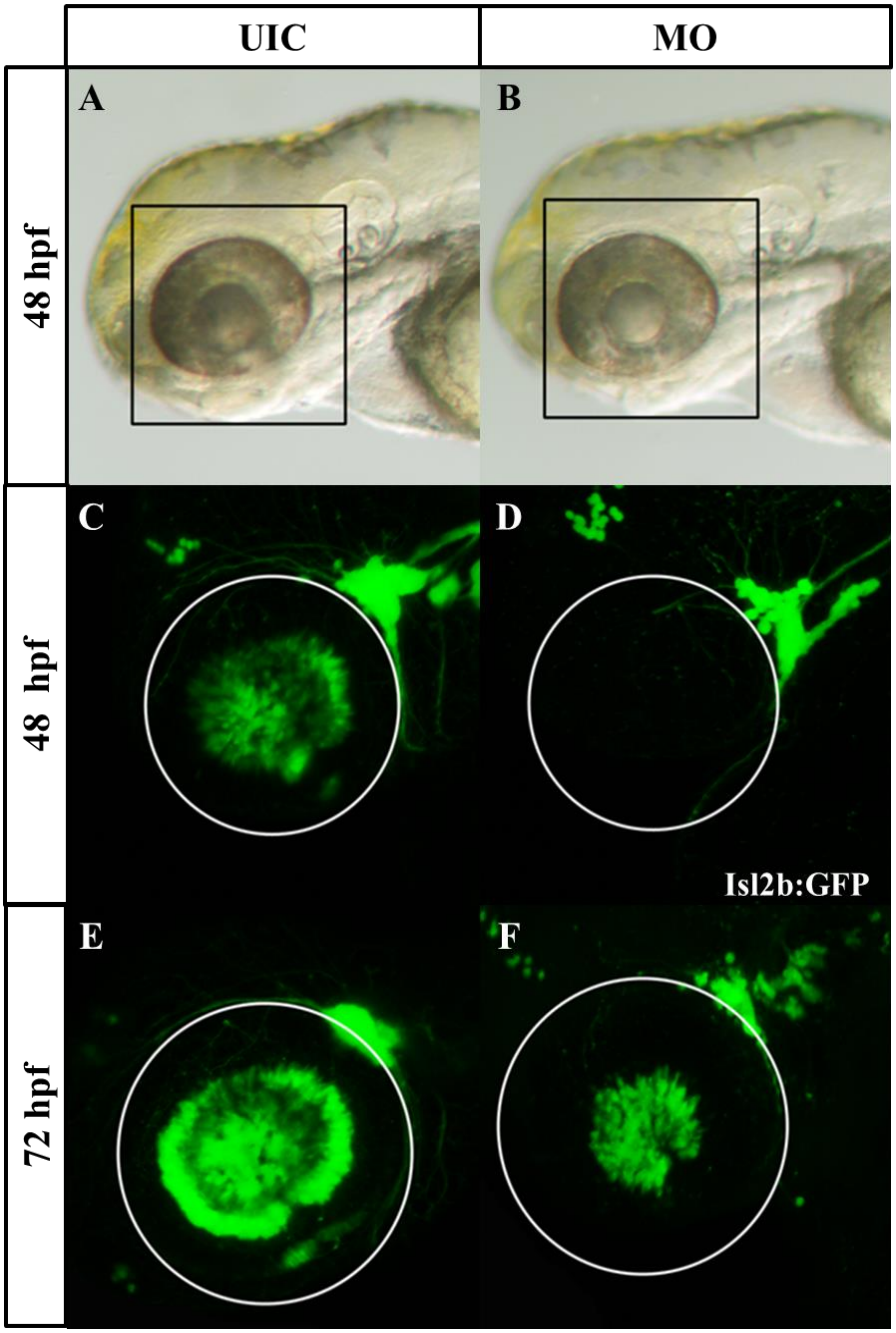

Figure 1.4.2. dcbld2 morphants have reduced differentiation of RGCs. While UIC (A) and morphants (B) do not seem to have any major gross morphological differences, RGC differentiation is hindered in the morphants (D, F). RGCs in the UIC begin to differentiate by 28 hpf and the visual system is complete by 72 hpf (C and E). Morphants often showed a complete lack of differentiation at 48 hpf and would rebound minimally in the next 24 hours (D, E). Cranial ganglia, adjacent to the retina, developed normally in both cases.

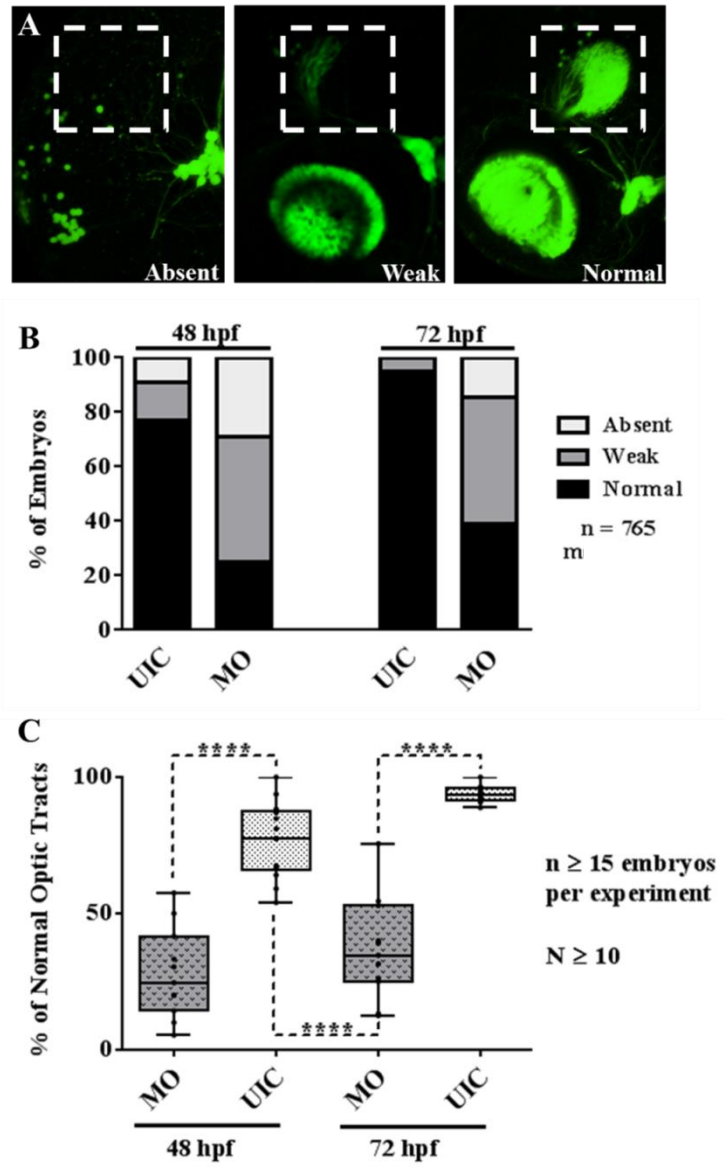

Figure 1.4.3. Morphant fish fail to develop normal optic tracts. Optic tract formation is scored on a basis of absent, weak, or normal (A). 77% of UIC (n = 696) have normal optic tracts at 48hpf, with 14% being weak, and 9% absent (B). By 72 hpf 95% of UIC (n = 451) have normal optic tracts, with 5% being weak, and less than 1% missing tracts (B). 25% of morphants at 48 hpf (n = 368) have normal optic tracts, 46% being weak, and 29% absent (B). At 72 hpf 39% of morphants (n = 309) have developed normal optic tracts, 46% have weak tracts, and 15% are still absent (B). By binning absent and weak together morphants can be compared to UICs by evaluating the percent of normal optic tracts. At 48 hpf morphants differ stastically from UIC (C, $P<0.0001$, unpaired Student's t test), and this result is consistent at 72hpf as well (C, $P<0.0001$, unpaired Student's t-test). In evaluating the chance that the morpholino is causing developmental delay, UIC at 48 hpf was compared with morphants at 72hpf (C, $P<0.0001$, unpaired Student's t-test). Given 24 additional hours to develop, morphants at 72 hpf still had less normal optic tracts than UICs at 48 hpf. Morphants received 3 ng injections and

dcbld2 Morphants Have Fewer Cells in the RGC Layer

Transgenic lines are fantastic for highlighting specific components, cells, or structures, but can be misleading as fluorescent intensities can change and not every embryo in a clutch is positive for the fluorescent tag. Therefore, to confirm the result in the evaluation of the optic tracts, UIC and morphant embryos were sectioned and DAPI stained to highlight nuclei. RGCs, identified by position within the retina and morphology, were counted to compare RGC layer cell number between UIC and morphants. Viewing of DAPI stained sections raised issues of lamination and eye size that will be considered in sections 1.4.5 and 1.4.6. It is important to note that when counting the cells in the RGC layer, some displaced amacrine cells are bound to be included, especially at the early developmental stages.

48 hpf UIC (Figure 1.4.5 A, n = 21) had a mean of 43 (±2.125) cells in the RGC layer, and 48 hpf morphants (Figure 1.4.5 B, n = 27) had a mean of 29 (± 1.482) cells in the RGC layer (Figure 1.4.5 A, B, C). The total cells in the RGC layer was statistically less in the 48 hpf morphants than the 48 hpf UIC (Figure 1.4.4 C, $P<0.0001$, unpaired Student's t-test). The 48 hpf time point showed the greatest proportional difference between UIC and morphants throughout developmental profile.

By 72 hpf the UIC embryos (Figure 1.4.5 D, n = 24) had 134 (± 3.316) cells in the RGC layer in comparison to morphants (Figure 1.4.5 E, n = 35) having 112 (± 3.373) (Figure 1.4.4 F). While the proportional difference in cells had decreased between the UIC and morphants, it was still significant (Figure 10 F, $P<0.0001$, unpaired Student's t-

test). By 8 dpf, the UIC embryos (Figure 1.4.4 G, n = 22) had 159 (± 1.820) cells in the RGC layer. The morphant fish at 8 dpf (Figure 1.4.4 H, n = 37) have failed surpass the UIC at 72hpf with the mean number of cells in the RGC layer being 119 (± 5.9). Not surprisingly, the difference between 8 dpf UIC and morphants with regard to cells in the RGC layer is statistically significant (Figure 1.4.4 I, $P<0.0001$, unpaired Student's t-test).

Comparing the UICs at 72 hpf with UIC at 8dpf and morphants at 72 hpf and 8 dpf, leads to interesting results. While the visual system is largely completed by 72 hpf, the eye is still undergoing synaptic refinement, and growing in size with late differentiating cells filling out the expanding eye (Gilbert, 2014). This can be seen in the significant change in cell numbers in the RGC layer from the 72 hpf UIC to the 8 dpf UIC (Figure 1.4.4., F and I). This change is not reflected in the morphant fish. From 72 hpf to 8 dpf the eye does not change significantly, with only a few more retinal ganglion cells appearing over the late developmental window (Figure S2, $P>0.05$, unpaired Student's t-test).

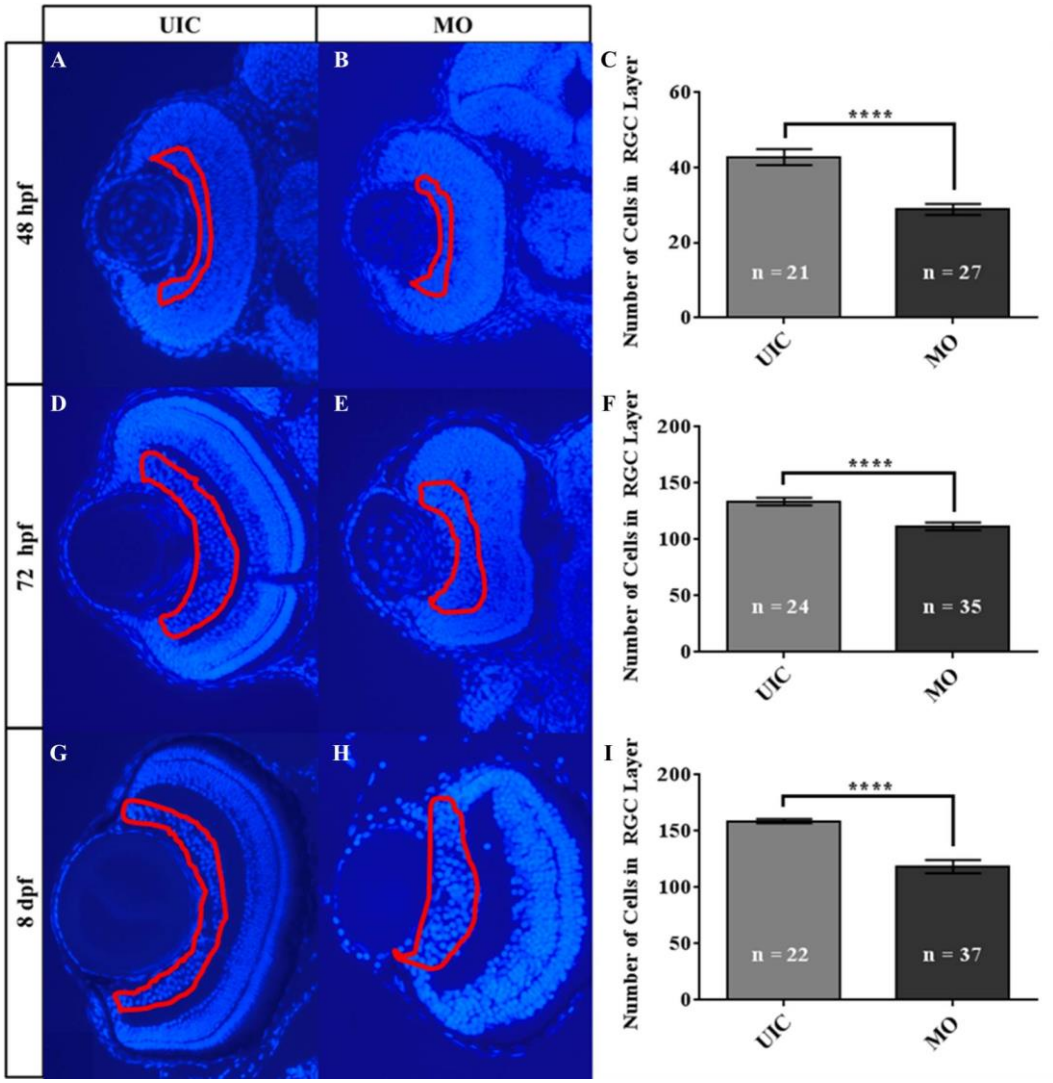

Figure 1.4.4. dcbld2 morphants have a reduced number of cells in the RGC layer. Total cells in the RGC layer (red outline) at 48 hpf for UIC (A, n = 21) was 43 (±2.125), contrasting the morphants (B, n = 27) who had 29 (± 1.482). The defiency in cells was signifigant (C, P<0.0001, unpaired Student's t-test). At 72 hpf the UICs (D, n = 24) had increased to 134 (± 3.316) cells in the layer. Morphants (E, n = 35) also exhibited an increase to 112 (± 3.373) and while the proportional difference between the two groups had decreased the difference was still significant (F, P<0.0001, unpaired Student's t-test). Cell numbers in the RGC layer in 8 dpf UICs (G, n = 22) became very consistent with a mean of 159 (± 1.820). Morphants (H, n = 37) did not recover any further and remained close to their cell numbers at the 72 hpf time point with a mean of 119 (± 5.9) at 8 dpf. The difference between the UIC and morphants remained significant (I, P<0.0001, unpaired Student's t-test). Scale bar represents 50 µm.

Receptor Knockdown Disrupts Retinal Lamination

The phenotype first noticed in the deficiency of RGCs and normal optic tracts was a very specific evaluation of retinal development. To characterize the phenotype beyond RGC differentiation, UIC and morphant sections were hematoxylin and eosin stained (H&E) stained to gain a more comprehensive picture of eye structure.

At 48 hpf ,the UIC has begun differentiation of the eye and a good population of RGCs is present with a border just adjacent which will become the inner plexiform layer (Figure 1.4.5 A). By 72 hpf, the UIC retina has become fully laminated with clear distinction of the RGC layer the IPL, INL, OPL, ONL, and RPE (Figure 1.4.5 C). By 8 dpf the eye has slightly increased in size and the lamination has become more distinct, but retinal development is largely complete (Figure 1.4.5 E).

H&E sections revealed morphant retinas were not only failing to develop or differentiate properly, but they also had defects in lamination. Morphant fish at 48 hpf had very little RGC differentiation, and lamination was often completely absent (Figure 1.4.5 D). By 72 hpf, some RGCs in the morphants had begun to differentiate, but lamination was still absent. This was particularly evident at the border between the retinal ganglion cells and what seems to be undifferentiated precursors (Figure 1.4.5 D). At 8 dpf, the morphants had generated a small layer of differentiated retinal ganglion cells adjacent to the retina, but lamination was incomplete (Figure 1.4.5 F). The IPL has opened next to the RGCs and it seems the INL has partially formed, but overall, the 8 dpf morphant retinas are lacking in organization and the normal diversity of cell types

(Figure 1.4.5 F). 8 dpf is well-beyond the developmental window for retinal differentiation and lamination to occur, suggesting that the developmental program is not simply delayed in the morphant fish.

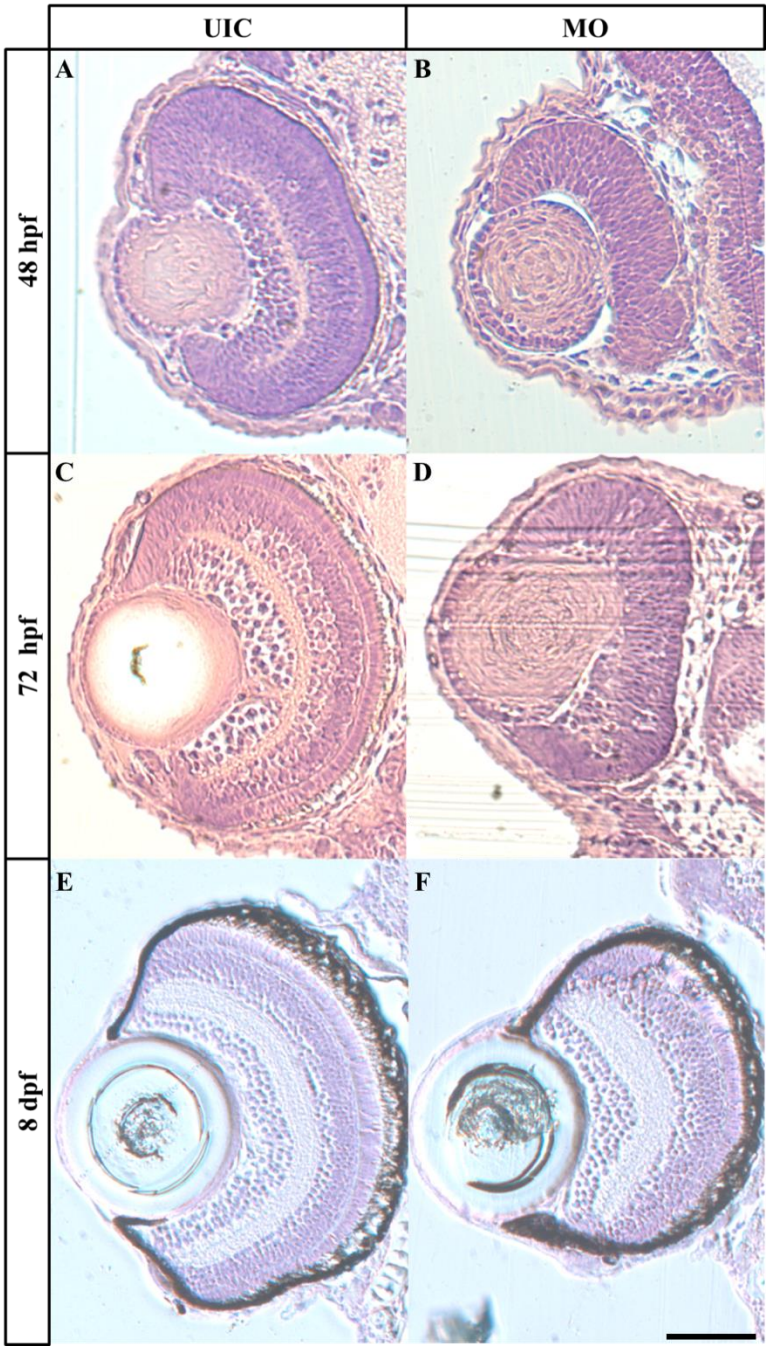

Figure 1.4.5. dcbld2 knockdown disrupts lamination of the retina. Lamination occurs normally in UIC, progressing from RGC differentiation and IPL formation at 48hpf (A), to complete lamination and organization at 72 hpf (C), to a fully resolved retina at 8 dpf (E). Progression is hindered to the point of failure in morphants, with little to no apparent RGCdifferentiation at 48 hpf (B). By 72 hpf some retinal ganglion cells have differentiated, but lamination is all but absent (D). At 8 dpf more RGCs have differentiated and the inner plexiform layer has opened, but lamination is still incomplete at a point when no further development will occur (F). Scale bar represents 50 µm

dcbld2 Morphant Fish Have Smaller Retinal Areas

When first assessing the phenotype in the transgenic fish, it appeared there were no gross morphological differences in UIC and morphant eyes. To a degree this was true as the major structures of the eye developed in both groups. As the phenotype was characterized from a broad perspective, looking at overall structure and organization it did seem that the retinal tissue itself was less abundant. To confirm this result, eye areas of UIC and morphants were measured at 48 hpf, 72 hpf, and 8 dpf.

Eye area at 48 hpf for UICs (Figure 1.4.6 A and C, n = 64) was 41,316 μm^2 (±732.5) and for morphants (Figure 1.4.6 B and C, n = 86) was 32,252 μm^2 (±1248). This difference was significant and somewhat expected after observing size differences a number of times in DAPI-stained retinas (Figure 1.4.6 C, $P<0.0001$, unpaired Student's t-test).

The eye is still growing in the 48-72 hpf age range and this was reflected in the size differences of both groups. The 72 hpf UICs (Figure 1.4.6 E and G, n = 87) grew approximately 37% increasing, to a mean area of 56,500 μm^2 (±363.4). The morphants (Figure 1.4.6 F and G, n = 74) grew approximately 34% increasing in retinal area to 43,212 μm^2 (±962.5). While the difference in retinal area between UIC and morphants at 72 hpf was significant (Figure 1.4.6 E, F, and G, $P<0.0001$, unpaired Student's t-test), the percent growth seen in the eyes was not significant (Figure S3, $P>0.05$).

By 8 dpf UIC (Figure 1.4.6 I, n = 22) retinal area had reached 66,317 μm^2 (±1,023) and morphant's eye area had reached 55,126 μm^2 (±1831). Again, the difference

between UIC and morphant retinal areas was significant (Figure 1.4.6 K, $P<0.0001$, unpaired Student's t-test). Reviewing percent growth from 48 hpf to 8 dpf, UIC fish (n = 65) increased their overall retinal size by 60.5% (±1.77) and morphants (n = 87) by 70.1 % (±3.87). While, percent of retinal size increase was larger in the morphants than the UICs, the morphant retinal areas were still smaller than the UIC overall.

After observing smaller retinal areas in the morphants throughout development, it became important to assess the specificity of this apparent tissue loss. If tissues derived from multiple germ layers were all proportionally smaller, it would not leave much room to talk about the specificity of our phenotype. To address this potential problem, lens area was measured as well. The lens is derived from surface ectoderm whereas the retina forms from neural ectoderm, allowing us to delineate effects of dcbld2 knockdown, if any, within these two distinct tissue types.

Lens area in 48 hpf UIC (Figure 1.4.6 A and D, n = 32) was 3,821 μm^2 (±78.45) and morphants (Figure 1.4.6 B and D, n = 35) 3,838 μm^2 (±102.4). The difference was not significant, in fact, the mean lens areas in morphants was larger than UIC at 48 hpf (Figure 1.4.6 D, $P>0.05$, unpaired Student's t-test). This lack of difference trend continued with lens areas being very similar between UIC (Figure 1.4.6 E and I, n = 19, n = 12) and morphants (Figure 1.4.6 F and J, n = 19, n = 12). No significant difference was detected at either 72 hpf or 8 dpf when comparing UIC to morphants (Figure 1.4.6 H and L, $P>0.05$, unpaired Student's t-test).

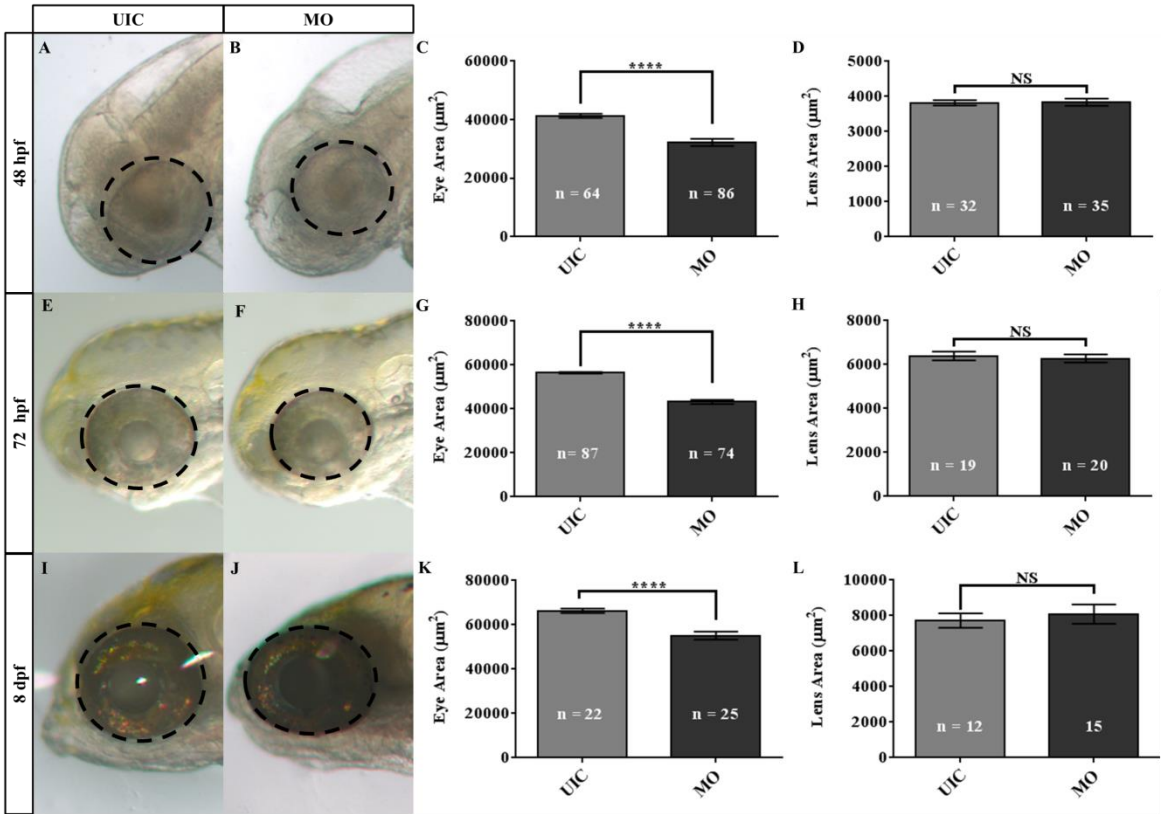

Figure 1.4.6. Morphant zebra fish have smaller eye area throughout develpment. 48 hpf UIC (A and C, n = 64) have smaller retinas than morphants (B and C, n = 86) at the same time point (C, P<0.0001, unpaired Student's t-test). At 72 hpf the pattern remained with UIC (E and G, n = 87) having larger retinal areas than morphants (F and G, n = 74, P<0.0001, unpaired Student's t-test). While morphants (J and K, n = 25) did slightly recover some by 8 dpf, their retinal area was still significantly smaller than UIC (I and K) at the same time point (K, P<0.0001, unpaired Student's t-test). Interestingly the lens, derived from surface ectoderm, was not different between UICs (D, H, and L, n = 32, n = 19, n = 12) and morphants (D, H, and L, n = 35, n = 20, n = 15) throughout development (D, H, and L, P>0.05, unpaired Student's t-test).

DISCUSSION AND FUTURE DIRECTIONS

In Situ Hybridization

In situ hybridization demonstrated that dcbld2 mRNA is transcribed in the developing nervous tissue of the zebrafish. The head and the eye exhibited the most abundant binding of the anti-sense probe, with apparent localization in certain eye and brain regions (Figure 1.4.0 B-G). mRNA transcript location was expanded at 48 hpf, with anti-sense probe binding further down the trunk of the embryo and becoming diffuse in the posterior regions of the organism (Figure 1.4.0 C). This result was consistent with data showing that the dcbld2 splice site morpholino, as previously described (O'Connor, Salles et al. 2009), caused intersegmental vessels to form improperly, often not fully projecting dorsally (Nie, Guo et al. 2013). Clearly, dcbld2 has functions in other regions of the developing zebrafish. Staining at 48 hpf is most likely expanded due to these functions, however, the staining is not specific enough for a confident statement about localization to be made.

With dcbld2 being known to play a role in angiogenesis why, then, is it not seen globally throughout zebrafish development? Due to the proposition that dcbld2 was involved in nervous tissue development, time points selected for *in situ* hybridization were based upon the neuronal differentiation timeline for the zebrafish eye and were 24, 48, and 72 hpf. This inquiry window does not overlap the primary window of vessel and artery development. At 30 hpf the zebrafish has developed its arteries, most vessels, and circulation has begun (Kimmel, Ballard et al. 1995). By 36 hpf the embryo has strong

circulation and its vasculature is largely complete, with the exception of intersegmental vessels and the caudal artery (Kimmel, Ballard et al. 1995). By focusing on the developmental timeline of nervous tissue, we may have missed dcbld2 mRNA localizations related to vasculature. dcbld2 has also never been characterized during early development. Furthermore, the data supporting dcbld2's role in processes like angiogenesis was collected in adult or postnatal organisms. *In situ* hybridizations at earlier time points would be important in determining what role DCBLD2 plays in development of the vasculature.

Given DCBLD2 was found to interact with Crk and CrkL is developmentally relevant, it was expected that the pair would co-localize during neuronal development. CrkL is known to be conserved across taxa, an attribute that is not surprising due to the critical nature of the adaptor in different processes (Figure S1). Logic then follows, that CrkL must be acting within a similar area as DCBLD2 for their interaction to be physiologically pertinent. While data is limited, CrkL has been showed to present the same neuronal mRNA localization pattern as DCBLD2 (Figure S1). CrkL mRNA localization in combination with *in situ* hybridization data of DCBLD2 supports the notion of the receptor having a role in development of the nervous system.

Morpholino Considerations

Transcript knockdown resulted in a number of developmental defects but it is key that considerations be made when interpreting these results. Morpholino effect is attenuated over time as the inhibitory RNA is partitioned repeatedly by dividing cells.

Most morpholino induced phenotypes have been identified within 72 hpf, but some have been observed as late as 5 dpf (Bill, Petzold et al. 2009). Generally, morpholinos are considered to be effective up to 6 dpf. Other factors influencing the efficacy of morpholinos include turnover time of target protein, percentage of protein knocked down, and the amount of functional protein needed to have proper function. It is important to note that in all experiments dcbld2 knockdown was close to 50% (Figure 1.4.0 E), and complete knockdown of the transcript caused severe defects (Figure 1.4.0 A, B, and D).

dcbld2 Knockdown Affects RGC Differentiation and Optic Tract Formation

The first observed phenotype was in the transgenic *Isl2b:GFP* fish line. Embryo's injected with dcbld2 morpholino were not having RGCs undergoing differentiation at the same time and or rate as wildtype fish (Figure 1.4.1 D and F). This resulted in optic tracts projected by the RGCs being weak or absent in morphant fish (Figure 1.4.3 B and C). The difference in normal optic tracts in UIC versus morphants was significant and reproducible (Figure 1.4.3 C).

Cell division in early neuroblasts is rapid, building up progenitor pools to be supply for the differentiation of the entire retina. If dcbld2 knockdown was affecting proliferation and therefore overall precursor numbers, it would be logical that there would also be less RGCs. However, when total cell numbers were counted in DAPI sections, UIC and morphants showed no difference at 48 and 72 hpf (Figure S2). Dcbld2 has been shown to modulate signals from growth factors to effectuate proliferation. For example, Dcbld2 inhibits PDGF induced proliferation and migration responses in

VSMCs (Guo, Nie et al. 2009). In contrast, VEGF proliferation and migration responses in HUVECs are promoted by DBCLD2 (Nie, Guo et al. 2013). Reduction or deletion of the receptor in adult zebrafish and rat resulted in reduced growth capability of the vasculature (Nie, Guo et al. 2013).

The evidence from work in vasculature shows DCBLD2 can act as a scaffold and transduce signals from different factors. Depending on the signal and the complexes that form as a result, cellular responses will differ. However, the only factors that have been investigated are largely irrelevant in terms of zebrafish retinal histogenesis. Additionally, retinal precursor cell numbers were not different between UICs and morphant fish. Presumably, signals in the early retinal environment that affect precursor proliferation like *shh*, are not interacting with dcbld2 to affect proliferation.

However, DCBLD2 has been shown to affect cellular migrations and has been found in association with molecules influencing cellular guidance (Aten, Redmond et al. 2013; Guo, Nie et al. 2009; Nie, Guo et al. 2013). Function in a migration context is more consistent with the lack of RGC differentiation that was observed. RGCs could be undergoing interkinetic nuclear migration improperly and missing the initial surge of *shh* from the ventro-nasal pouch that instructs differentiation. Another possibility is differentiation is occuring at the apical surface, but RGCs are making errors in migration back to the basal surface. While the evidence points towards a migrational function for dcbld2 in retinal development, additional experiments need to be performed to confirm this proposition. Thymidine dating would be a strong experiment to visualize the order in which neurons are being born and if those neurons are migrating from the apical surface

to their proper location within the retina.

Other logical rationale, derived from the first experiment, would be the disturbance of the internal constituents of early precursors. dcbld2 knockdown is somehow affecting the promoter for the *Isl2b:GFP* or the GFP protein itself, and or loss of the receptor is affecting a higher signaling cascade that derails embryogenesis before differentiation. Internal constituents that drive symmetrical or asymmetrical division in developing neuroectoderm are largely controlled by lateral inhibition. This process is mediated by the Delta-Notch pathway that regulates proliferation and specification in the developing nervous system (Appel, Givan et al. 2001). Proliferation and differentiation of the nerves that innervate the face, the cranial ganglia, is also controlled by lateral inhibition. However, the cranial ganglia appear to differentiate properly relative to UIC (Figure 1.4.2 C-F) and can be seen in an area directly adjacent to the retina (Andermann, Ungos et al. 2002). The cranial ganglia are also under the influence of the hierarchical bHLH transcription factor gradients that specify tissues in the embryo (Andermann, Ungos et al. 2002). The seemingly proper development and differentiation of the cranial ganglia suggests the dcbld2 has a specific role in retinal differentiation at the 48 and 72 hpf time points.

The qualitative evaluation of optic tracts (Figure 1.4.2 B) highlighted that although RGC differentiation and optic tract formation were deficient early in development, they were trending toward normal. It was necessary to go beyond 72 hpf to determine if the morpholino effects were permanent or would be alleviated in time.

dcbld2 Morphants Have Fewer Cells in the RGC Layer

To gain perspective on RGC differentiation, DAPI-stained sections were created to look at numbers and positioning of cell nuclei with respect to the RGC layer. At 48 hpf a small proportion of cells in the RGC layer will be displaced amacrine cells and this should be noted. The dcbld2 morphants had fewer cells in the RGC layer at 24 hpf, 48 hpf, and 8 dpf (Figure 1.4.4 C, F, and I).

RGCs are the first retinal neurons to differentiate and are a hinge point for retinal differentiation overall. RGCs exit the cell cycle and differentiate terminally beginning at 28 hpf (Sernagor 2006). RGCs are stimulated to differentiate by a wave of *shh* expression within the ventro-nasal patch (Stadler, Shkumatava et al. 2004). It is difficult to observe at 48hpf, as the retina is just beginning to take on its laminar structure, but by 72hpf and 8 dpf the difference in the RGC layer is clear (Figure 1.4.4 B, E, and H). RGCs surrounding the retina in morphants are less abundant and are not packed tightly. However, the DAPI section counts do match the dcbld2 knockdown results in the *Isl2b:GFP* transgenic, with a deficient but properly differentiated RGC population surrounding the retina. Most morphants had some properly differentiated RGCs, denoted by the projection of axons to the optic tectum.

The reduced RGC cell population does support the idea that s*hh* is being expressed in the ventral nasal pouch, allowing for differentiation of the cells residing in that zone. The lack of cells in the RGC layer overall, points to the idea that possibly migration mechanisms of precursors was affected by dcbld2 knockdown. The effect was

also permanent, as by 8 dpf zebrafish have completed eye development and will not have large numbers of precursors differentiating into RGCs. It is important to note that stem cells from the ciliary marginal zone could fill in some of these gaps. Stem cells differentiating form the ciliary marginal zone could also account for the recovery seen in the 8 dpf morphant embryos.

Knockdown efficiency especially is important to consider when interpreting these results. dcbld2 was knocked down by 50% and so functional receptor is still present. While we see a reduction in the number of cells in the RGC layer, it would be odd to see a complete loss overall. The RGC cell layer does not, however, have 50% fewer cells either. It may seem rational that a 50% reduction in protein would lead to a corresponding drop in the observable phenotype, but there are many variables that would influence this relationship. As stated previously, the morpholino loses efficacy over time which would result in an increasing percentage of functional protein over development. Also, the function of the DBCLD1 homolog in zebrafish is relatively unknown and there could be a level of compensation reducing the knockdown effect of dcbld2. Compensation could include reducing the effectiveness of the morpholino, partially rescuing phenotypes caused by loss of dcbld2, and increased rate of recovery from morpholino affects among others.

Receptor Knockdown Disrupts Retinal Lamination

The lamination defects thought to be observed in the DAPI-stained sections were confirmed with H&E staining of 48 hpf, 72 hpf, and 8 dpf embryo sections (Figure 1.4.5

A-F). Retinal lamination, comprised by the INL, IPL, ONL, OPL, RPE, and defined by the different neuron types residing in specific positions, was disrupted by dcbld2 knockdown. Lamination was all but absent in the 48 hpf morphant (Figure 1.4.5 B). The 72 hpf morphant embryo (Figure 1.4.5 C) has a very poorly-defined RGC layer. By 8 dpf the embryo had developed a scant but visible RGC layer, an IPL, and the beginnings of an ONL (Figure 1.4.5 F). Laminar definition dissipates quickly from the ONL, and the three outer layers are muddled without clear definition between the cell types (Figure 1.4.5 F).

Lamination is orchestrated, as discussed in the introduction, by a complex network of early inductive cues and differential expression of transcription factors activated by inductive signals. Precursors are also responding to factors that are being expressed by post-mitotic neurons. Post-mitotic RGCs express *shh*, creating a feedback loop to amplify differentiation and yet inhibit adjacent cells from taking on a similar cell fate (Stadler, Shkumatava et al. 2004). Post-mitotic RGC secretion of shh is matched by another wave of s*hh* expression from the ventral-nasal pouch region (Stadler, Shkumatava et al. 2004). The second wave of shh enables the cells of the IPL, the amacrine, bipolar, horizontal cells, and muller glia to differentiate (Stadler, Shkumatava et al. 2004). The H&E stained sections show weak, but successful, differentiation of cells in these layers and thereby partial lamination of the retina (Figure 1.4.5 F).

Looking closely at the 8 dpf retina in both the DAPI (Figure 1.4.4 H) and H&E (Figure 1.4.5 F) sections, reveals something more. The DAPI-stained sections make lamination easy to see because the synapse layers lack nuclei. In the 8 dpf and even in the

72 hpf (Figure 1.4.4 E and H), you can see the outline of all the major layers in the retina. These layers do not resolve into the organization seen in the UIC and it is clear that cells are misplaced throughout the layers. The H&E stained sections tell a similar story. If the H&E sections are examined closely, it appears that by 8 dpf all of the cell types have been born in the morphant (Figure 1.4.5 F). The laminar layers are not completed and cells are misplaced, but it does seem that at least some of each cell type has differentiated. Cell types within the layers were identified by morphology and position alone, and a more comprehensive technique like immunohistochemistry would be needed to ensure cell identity.

dcbld2 Morphant Fish Have Smaller Retinal Area

Morphant zebrafish do not have gross morphological malformations of the eye, but eye areas are smaller than UIC. Eye area (um^2) was significantly different throughout development (Figure 1.4.6 A-K). Eye size is largely based on cell proliferation, death, orientation, and packing. Total retinal cells at 48 hpf and 72 hpf (Figure S2) were the same, and so precursor proliferation and programmed cell death do not seem to be effected. Orientation or organization of cells is an important factor in eye size. If the eye develops normally, the laminated organization is larger than when lamination defects are present. Multiple studies have shown that a loss of lamination is almost always connected to a loss in eye size, barring side effects (Catalano, Raymond et al. 2007; Kennedy, Stearns et al. 2004).

While the loss of lamination was the most likely culprit of reduced eye size,

comparing lens area gave us another chance to highlight the specificity of the morpholino. Lens derives from surface ectoderm and retina from neural ectoderm. If dcbld2 was only affecting nervous tissue development in the zebrafish eye, there should be no difference between morphants and UICs with regard to lens area. Lens areas were not significantly different between the UIC and morphants at any time point (Figure 1.4.6 D, H, and L). The UICs and morphants were also compared on the ratio of retinal diameter to lens area. Essentially, this test tightens the stringency on determining if the eye size differences being observed are specific to the tissue or you have a global effect. The ratio of retinal diameter to lens area was significantly different at all three time points, showing that smaller retinal diameter was not associated with a smaller lens as well (Figure S2 C, D, and E).

Addressing Developmental Delay

Developmental delay can be an unintended effect of morpholinos, typically as a result of apoptosis (Ekker and Larson 2001; Robu, Larson et al. 2007). Additionally, we noticed that as development progressed the phenotypes observed in RGCs, optic tracts, and retinal lamination reduced in severity (Figure 1.4.2 D and F, Figure 1.4.3 B). Again, this could be a product of incomplete knockdown and morpholino attenuation. Close to 50% of dcbld2 is still functional in the developing embryo, yet we see a severe loss of lamination and optic tract formation early in development. Analysis was performed on previously collected data, and current experiments were carried out to 8 dpf to ensure developmental delay was not our major phenotype.

Total retinal cell counts at 48 and 72 hpf show that UIC and morphants do not differ significantly, and so apoptosis is probably not occurring at higher rate in morphants (Figure S2 A and B). The utilization of the P53 cell death cascade blocking morpholino also indicates off-target apoptosis is not playing a role in the phenotype (Figure 1.4.1 A, B, and F) Comparison of 72 hpf morphants to UIC at 48 hpf showed that when morphants had an additional 24 hours to develop they still had less normal tracts than UIC (Figure 1.4.3 C). Additionally, comparing the ratio of retinal diameter to lens area between UIC and morphants all the way out to 8 dpf (Figure S2 C, D, and E) revealed a difference in retina diameter without a corresponding change in lens size. Because these structures are derived from different parent tissues, this comparison highlights the phenotype specificity.

In combination, the evidence compiled, provides a strong case refuting developmental delay as the primary morphant defect. Furthermore, while morphant fish did show a recovery trend, 8 dpf fish had lasting phenotypes that would not be alleviated over time. Despite the fact approximately half of dcbld2was still functional and the morpholino efficacy was constantly reducing, we saw permanent phenotypes caused by lack of the receptor.

Future dcbld2 Zebrafish Studies

The most important experiment to wrap this study together is the WT rescue of dcbld2 knockdown or knockout. A successful WT RNA rescue of the phenotype would provide strong evidence for the specificity of the morpholino and the phenotypes observed. A validation technique such as an internal ribosomal entry site or western blot

to confirm or detect the translation of RNA into protein would be necessary. The Y7F DCBLD2 mutant RNA could also be injected to determine if the YxxP motifs are required for proper rescue. A failed rescue would indicate that the DBCLD2 signaling cascade, at least in the context of retinal development, requires the CrkL adaptor protein to propagate the signal.

A dcbld2 knockout/knockdown zebrafish line would also be a great tool in investigating dcbld2 function. The CRISPR/CAS9 system is being employed in an attempt to generate this mutant. If the previous morpholino work is validated and knockout of dcbld2 is embryonic lethal, fish will have to be maintained as heterozygotes or conditional knockouts could also be generated. The embryos from a heterozygote cross could also be injected with WT RNA after fertilization to allow for survival and still gain an understanding of the knockout results.

Knockdown of dcbld2 by a half led to severe retinal defects which were attenuated over development but were permanent. The lasting effects of the early knockdown were not addressed from a behavior point of view. Do the reductions in RGC differentiation and lamination of the eye cause vision abnormalities in the fully developed zebrafish? The vertebrate optokinetic response is a behavior in which the eye will continually track a moving object across the field of view (Zou, Yin et al. 2010). Visual assays exploiting this behavior to evaluate visual function in zebrafish have been widely used and well characterized (Zou, Yin et al. 2010). This technique could be utilized to determine if lasting effects of dcbld2 knockdown inhibited visual function.

Future DCBLD2 Biochemical Studies

A persistent goal of the DCBLD2 studies has been to identify the ligand for the receptor. DCBLD2 has been shown to modulate responses from factors like VEGF and PDGF and complex with the VEGFR2 and SEMA4B (Guo, Nie et al. 2009; Nagai, Sugito et al. 2007; Nie, Guo et al. 2013). However, none of these potential candidates resulted in DCBLD2 phosphorylation at the CrkL-SH2 YxxP binding motifs. The only molecule shown to induce DCBLD2 phosphorylation at the YxxP motifs is the constitutively active mutant form of the epidermal growth factor receptor (*EGFRvIII*) (Feng, Lopez et al. 2014). DCBLD2 phosphorylation by EGFRvIII is relevant to cancer studies as it is claimed to promote tumorigenesis, but does little to help us understand the normal physiological role of DCBLD2 (Feng, Lopez et al. 2014). Studying the receptor in different types of cancer is difficult because DCBLD2 has been shown to have widely differing expression levels and the whole system is essentially aberrant (Feng, Lopez et al. 2014). DCBLD2 could simply have been commandeered by the aberrant signaling cascades and used as a scaffolding to propagate cancer progression signals. To test this finding, EGF stimulation of DCBLD2 transfected HEK293 cells was carried out, but multiple experiments never showed EGF induced DCBLD2 phosphorylation.

Further binding studies will be needed to identify a true ligand(s) for DCBLD2, and also to determine other binding partners for the receptor. It is clear that the receptor can propagate a variety of signals and this is most likely accomplished through interactions with different ligands and or downstream signaling partners. Stable isotope labeling in cell culture (SILAC) in combination with H_2O_2 stimulation would be a viable

approach to identify new binding partners of DCBLD2. Mass spectrometry would need to be used in order to identify proteins that bound to phosphorylated, but did not bind to non-phosphorylated DCBLD2. The Y7F would be a strong control as it would highlight proteins that might bind, but not at the CrkL-SH2 YxxP motifs. Identifying downstream binding partners of DCBLD2 other than the Crk/L family adaptor proteins would allow for insight into the differential signaling capability of the receptor.

C3G has been highlighted as a possible downstream effector of DCBLD2, but there is no evidence directly linking the receptor and the GEF. To assess this relationship a cell culture experiment in which DCBLD2-FLAG and C3G and DCBLD2 Y7F-FLAG and C3G were co-transfected into E1A-transformed Human embryonic kindney (HEK293). Cells would need to be stimulated with H_2O_2 to induce phosphorylation. Lysates from WCE and FLAG-immunoprecipitations could be blotted for α-FLAG, α-C3G, and α-pY to determine if DCBLD2 phosphorylation results in C3G phosphorylation (activation) and if the two proteins complex.

CONCLUSIONS

DCBLD2 Could Signal Through C3G and Rap1 to Regulate N-Cad Expression

DCBLD2 knockdown affects cell number in the RGC layer, retinal lamination and size, but does not seem to be altering precursor number. The explanation or rationale most consistent with the evidence surrounding DCBLD2 function is that the receptor mediates neuronal precursor interactions with each other or with the matrix. Due to the complexity of retinal differentiation and development, this supposition opens up a number of doors.

One possibility for the phenotypes observed could have been improper cellular adhesion and migration. In retina development a critical molecule is neural cadherin-2 (N-cad), a transmembrane protein that facilitates $Ca2^{+}$ dependent cell adhesion and migration in addition to cell to cell signaling and cell to matrix signaling (Sernagor, 2006). N-cad is required for proper precursor migration and subsequent retinal development (Sernagor 2006). N-cad is expressed by all precursors and is under the regulation of Rap1, a small GTPase that regulates adhesion to N-cad and its expression at the cell surface (Jossin, 2011; Sernagor, 2006). Activation of Rap1 increases cell surface expression of N-cad (Jossin and Cooper 2011). While it is not clear how Rap1 directly regulates N-cad, it is proposed that Rap1 mediates vesicle trafficking between the ribosome and plasma membrane (Jossin and Cooper 2011). Rap1 is activated by the GEF C3G, and it has been shown that an activator of C3G is the Crk-family adaptor proteins (Ballif, Arnaud et al. 2004). C3G is recruited to the membrane by the SH3 domain of Crk

family adaptor proteins, where it becomes activated via phosphorylation (Hattori and Minato, 2003).

A potential model for the DCBLD2 receptor that is in line with current literature and the findings within this study can be assembled (Figure 1.6.0). It is important to note that while some of the interactions within pathway have been determined empirically, the overall pathway was guided by the phenotypes seen in the zebrafish model. The DCBLD2 receptor is clustered by a potential ligand. Phosphorylation occurs as a result of clustering; kinases at the plasma membrane or associated with the receptor are being brought in close enough proximity to relieve auto inhibition (Figure 1.6.0). Activation of kinases, such as Fyn, causes C-terminal phosphorylation of the YxxP CrkL-SH2 binding motifs (Figure 1.6.0). CrkL binds to the receptor and then recruits C3G bound via its SH3 domain. C3G is activated via phosphorylation by SFKs at the membrane and activates Rap1 through its GEF activity (Figure 1.6.0). Rap1 then mediates expression of neural cadherin at the cell surface.

Following this line of logic, if DCBLD2 is knocked down, less CrkL will be recruited. Fewer C3G molecules will become activated, resulting in less active GTP-bound Rap1, therefore, reduced N-cad at the membrane. In zebrafish, mutation of the *ncad*2 locus causes a major reduction in neuroepithelial integrity in the developing nervous system (Malicki, Jo et al. 2003). Loss of functional N-cad also results in drastic neuronal patterning abnormalities in the retina and brain similar to those seen in the DCBLD2 knockdown (Malicki, Jo et al. 2003).

Rap1 has not been well characterized in zebrafish nervous tissue, although it has been shown to be indirectly involved in neural crest cell migration (Smolen, Schott et al. 2007). When Rap1b, an isoform of Rap1 in zebrafish, is knocked down the phenotype evaluated in vasculature is strikingly similar to DCBLD2 knockdown, ISVs fail to form properly exhibiting stunted angiogenesis (Lakshmikanthan, Sobczak et al. 2011; Nie, Guo et al. 2013). This potential pathway is largely based on previously completed studies and more work would need to be completed to validate specific interactions. For example, the activation of Rap1 can be accomplished by GEFs other than C3G (Stork and Dillon 2005). Also, it has not been directly shown that C3G is activated downstream of the DCBLD2 signaling cascade. The pathway presented here is just one possible interaction scheme that fits with the literature and evidence from this study.

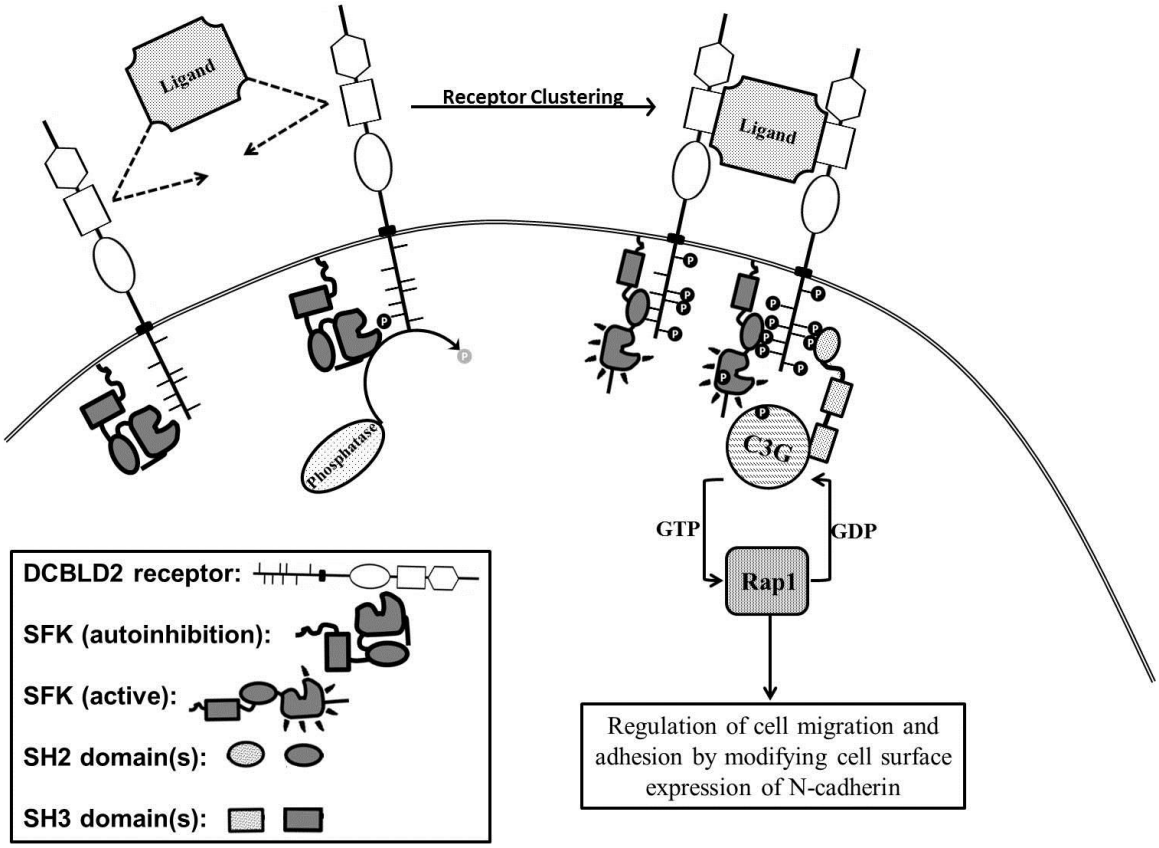

Figure 1.6.0. Clustering of DCBLD2 receptor leads to Rap1 activation and increased expression of N-cad at the membrane. When DCBLD2 is clustered in response to a ligand, kinases are brought into close proximity, allowing for autotransphosphorylation and relief of autoinhibition. Phosphorylation of multiple tyrosine residues in the YxxP motif on the C-terminus of DCBLD2 occurs as a result of increased kinase activity. The CrkL-SH2 domain is recruited to the phosphorylated tyrosines and, in turn, recruits C3G via its SH3 domain. C3G is phosphorylated at the membrane. Activation of C3G increases levels of active GTP-bound Rap1, increasing expression of N-cad at the membrane.

Evaluating DCBLD2 and CrkL Protein Association Networks

To validate if the previous model was viable and gain a more comprehensive perspective on the possible outcomes of signaling routed through the DCBLD2 receptor and the CrkL adaptor protein a bioinformatic tool known as STRING was employed (Jensen, Kuhn et al. 2009). The string software mines neighborhood, gene fusion, concurrence, co-expression, empirical, database, and text data to construct a network showing protein associations with the protein of interest (Jensen, Kuhn et al. 2009). It also produces the highest rated gene ontology (GO) terms, or functional descriptors, for that network cluster (Jensen, Kuhn et al. 2009).

DCBLD2 is in a small network as it is fairly novel, and study began on the receptor relatively recently. All of the known connections reported here were reflected in the network cluster, with a few additional uncharacterized proteins coming from large scale genomic studies (Figure 1.6.0 A). The top 5 GO terms for the DCBLD2 network were neurotrophin TRK receptor signaling, neurotrophin signaling, Fc-epsilon receptor signaling, MAPK signaling, and signal transduction by protein phosphorylation (Jensen, Kuhn et al. 2009). Neurotrophins, as mentioned in the introduction, are growth factors that are critical for neuron maintenance and development. The Fc-epsilon receptor refers binds to the fragment crystallizable region of an antibody and the signaling denotation indicates the ability to bind the epsilon form of that region. The multiple MAPK family members control numerous critical cell processes such as proliferation, differentiation, motility, and survival. Signal transduction by protein phosphorylation was confirmation of a function we already knew DCBLD2 to play, especially in association with the CrkL

adaptor protein. Overall, the DCBLD2 network does not allow us to conclude anything new definitively, but supports the potential role for the receptor in neuronal development context. It also highlighted the lack of direct evidence provided for DCBLD2's interaction with growth factors in the vasculature such as VEGF and PDGF (Jensen, Kuhn et al. 2009).

The CrkL network was more robust as the protein has been well characterized (Figure 1.6.0 B). Again, the proteins that were expected to be in the network were found, like C3G (RAPGEF1) and ABL1 (Jensen, Kuhn et al. 2009). The top 5 GO terms for the CrkL network were signal adaptor activity, protein binding, SH3 domain binding, SH3/SH2 adaptor activity, and protein kinase binding (Jensen, Kuhn et al. 2009). The GO terms returned for CrkL were supportive of its known role, but all very similar as its primary function is to simply link proteins via its SH2 and SH3 domains. The bioinformatics evaluation of the interactors in the DCBLD2 signal transduction pathway did support our proposed role for the receptor. However, a critical link is missing to connect the two networks and support our proposed model. The DBCLD2 network and the CrkL network (Figure 1.6.0 A and B) would be joined if a connection could be made from DCBLD2 to one of the downstream partners of CrkL. The natural candidate for investigation in this situation would be C3G (RAPGEF1), as we know it is activated when recruited to the membrane by CrkL and DCBLD2 phosphorylation can induce CrkL binding. This proposed experiment to link the two signaling networks is covered more thoroughly in future directions.

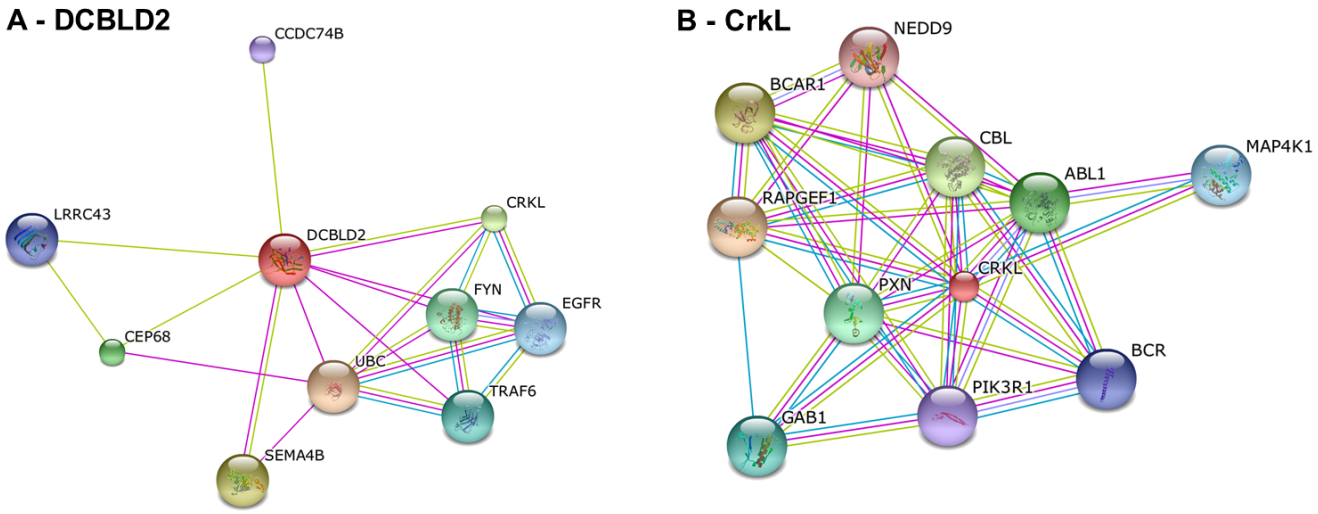

GO Terms:

1. Neurotrophin TRK receptor signaling pathway
2. Neurotrophin signaling pathway
3. Fc-epsilon receptor signaling pathway
4. MAPK cascade
5. Signal transduction by protein phosphorylation

GO Terms:

1. Signaling adaptor activity
2. Protein binding, bridging
3. SH3 domain binding
4. SH3/SH2 adaptor activity
5. Signal transducer activity

Figure 1.6.1. DCBLD2 receptor and CrkL adaptor protein association networks. Proteins are associated with the protein of inquiry (DCBLD2 or CrkL) by empricial evidence (pink), database submissions (blue), textmining (yellow), and homology (purple). DCBLD2 associations include known interacting partners like CrkL, Fyn kinase, and SEMA4B (A). The highest rated gene ontology (GO) terms, such as neurotrophin signaling and MAPK cascade, for the DCBLD2 network fell in line with the proposed novel function of the receptor (A). The CrkL adaptor protein network also fit with the known role of the protein, but no new interesting functionality was observed from the network (B). (Jensen, Kuhn et al. 2009)

Improper Migration or Division Could Compromise Eye Development

DCBLD2 has also been shown to modulate migration in response to growth factors (Guo, Nie et al. 2009; Nie, Guo et al. 2013). Unfortunately, not all of the signaling components and interactions involved in migration modulation have been determined. However, it is possible to take a step back and consider the overall effects altered migration would have on retinal precursors undergoing interkinetic nuclear migration. Contrasting information about whether DCBLD2 promotes or inhibits migration is less of a concern in this situation because normal migration will be disturbed either way. Precursors must migrate properly throughout interkinetic nuclear migration and then travel back down to the basal surface after mitosis and cell cycle exit has occurred. Proper migration is critical for precursors to encounter inductive signals for differentiation.

If knockdown of dcbld2 altered migration rates precursors could be losing synchronization between the cell cycle and position with regard to the apical and basal surfaces. This would result in precursors either undergoing division in the wrong positions or failing to migrate to the proper position after division has occurred. There is particularly true due to the fact that not only is precursor fate dictated by the extracellular environment, but also by the surrounding cells. Knockdown of dcbld2 could cause some presumptive RGCs to fail to reach their target destination in the central retina. The second wave of shh that is secreted by differentiated RGCs to inhibit other neuroblasts would be absent and the overall differentiation cascade would be interrupted. Loss of properly differentiated RGCs, and their inhibitive properties, results in precursors that

would normally become other neuron types of the eye taking on an RGC fate (Poggi, Vitorino et al. 2005). RGCs are the first neuronal cell to differentiate and if original populations were deficient due to knockdown of dcbld2, other precursors would then take on RGC cell fate. Late differentiating RGCs could account for the reduced, but relatively normal populations and could explain why optic tracts are late to turn on in the morphant fish. Precursors taking on RGC cell fate at an inappropriate time in may account for mispatterning in the other layers of the retina, as precursor pools have been abnormally allocated.

Precursor and cytoskeletal interactions are not only involved in migration, but also orient the cell. Orientation of precursors is important as partitioning of molecules, such as numb, to one pole or region of a dividing precursor leads to asymmetrical division and the birth of a neuron. There is strong debate about whether the mitotic spindle orientation with regard to the apical and basal surfaces influences whether a cell undergoes asymmetric or symmetric division (Sernagor 2006). While spindle location influence is controversial, it is clear that the plane of division is important in segregating internal constituents. Improper orientation of the cell due to loss of DCBLD2 mediated cytoskeleton interactions could cause improper inheritance of internal constituents and improper divisions. This would undoubtedly affect the timing of retinal differentiation as the normal differentiation wave would be disrupted.

There are many potential rationales that could be proposed to fit the phenotypes seen in the dcbld2 morphant fish. DCBLD2 function in concert with the adaptor protein CrkL points towards a role in migration for the receptor, especially in the context of

nervous tissue. However, the experiments presented here are the beginning stages of an *in vivo* functional analysis of DCBLD2 and more work is needed to fully characterize protein function.

Appendix A – DCBLD2 Antibody Clustering

Introduction

DBCLD2 contains a CUB domain which is prevalent in extracellular and transmembrane proteins. This domain is found in many critical developmental proteins and has been shown to interact with the LCCL domain another modular domain on DBCLD2 (Bork and Beckmann 1993). In recent work on a CUB domain containing protein that regulates cell adhesion, CDCP1 (CUB (complement C1r/C1s, Uegf, BMP1) Domain-Containing Protein 1), it was shown that antibody stimulation could induce SFK activation (Bork and Beckmann 1993). Antibody stimulation led to tyrosine phosphorylation of the receptor and phosphorylation of SFK at its 416 activation loop (Bork and Beckmann 1993).

Antibodies are at least divalent, allowing them to bind more than one receptor and cluster them together. If the finding indicated that high enough level of receptor expression is adequate to be an upstream activator of SFKs or the antibody is merely mimicking a ligand is unclear. However, as the mechanism of DCBLD2 was largely uncharacterized, the antibody treatment was a good approach to begin looking at the mechanism.

Materials and Methods

HEK 293 cells were grown in DMEM and underwent calcium phosphate transfection of DCBLD2-FLAG (ESDN-Flag) or the DCBLD2 Y7F-FLAG (ESDN Y7F-Flag) mutant and lysis as previously described (Aten, Redmond et al. 2013). Cells were treated with 2 ug/ml of antibody against the Factor V/VIII domain of DCBLD2 for twenty minutes, lysed as previously described (Aten, Redmond et al. 2013), and whole cell extracts were immunoblotted for α-Flag and α-pY (Aten, Redmond et al. 2013). Lysates from antibody treated and untreated cells were applied to a GST-CrkL-SH2 resin and immunoblotted for α-Flag as previously described (Aten, Redmond et al. 2013).

Results and Discussion

Antibody treatment resulted in phosphorylation of the WT, but not Y7F, DCBLD2 receptor in both whole cell extracts and α-Flag immunoprecipitations (Figure A1 A). The CrkL-SH2 pulldown showed that WT, but not Y7F, DCBLD2 could bind the SH2 domain when tyrosine phosphorylated by antibody stimulation.

Receptor clustering has been shown as a mechanism to activate signaling pathways by activating effectors like SFKs (Gale and Yancopoulos 1999). Transmembrane proteins with intracellular domains can facilitate this activation by acting as a scaffold for protein complexes. By providing phosphotyrosine sites for SH2 domain binding, SFK kinases, like FYN, are able to bind and activate by trans-autophosphorylation, relieving cis-auto inhibition (Lemmon and Schlessinger 2010). Activated kinases phosphorylate the receptors and potentially other proteins that are

recruited to the membrane by the SH2 binding sites (Figure 1.6.0).

While the receptor phosphorylation stimulated by antibody treatment hints at a mechanism for DCBLD2 activation, more work needs to be completed to fully characterize the mechanism. Mutants could be used to specify interactions and SILAC could potentially determine differential downstream effectors of antibody induced phosphorylation against another method of phosphorylation like H_20_2.

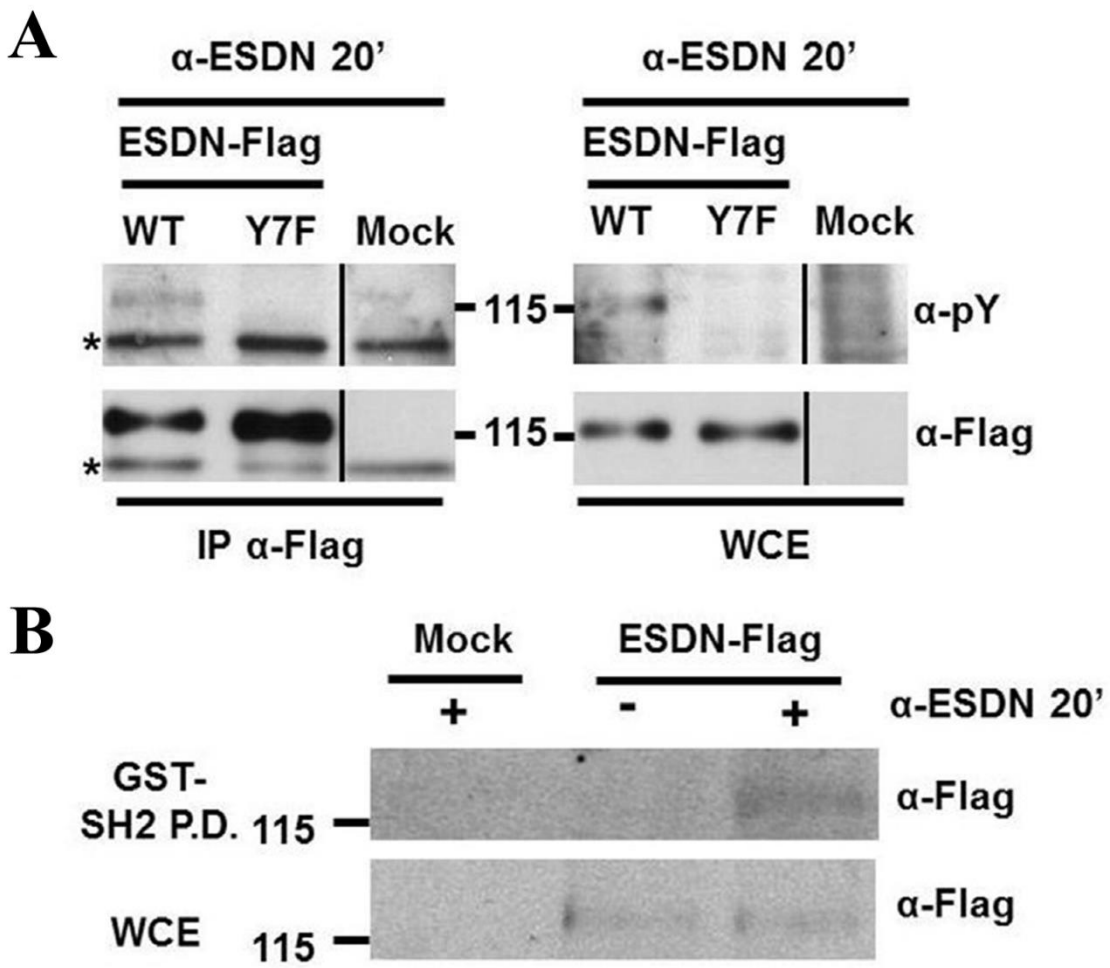

Figure A1. α-DCBLD2 antibody treatment induces tyrosine phosphorylation of the receptor and its interaction with the CrkL-SH2 domain. A twenty minute incubation with 2 ug/ml of α-DCBLD2 induces tyrosine phosphorylation of WT, but not Y7F, DCBLD2 (A and B). Phosphorylation of the receptor by antibody stimulation is sufficient to allow for the SH2 domain of CrkL to bind (C). Adapted from Aten, Redmond et al. 2013.

Appendix B – DCBLD1homologue can bind the CrkL-SH2 domain

Introduction

A bioinformatics screen was used to identify proteins that had CrkL YxxP SH2 binding motifs in high relative frequency. Binding motif frequency was based upon the the ratio of YxxP sites to total amino acids in the protein. Proteins that fell outside of one or two standard deviations were highlighted as proteins of interest due to their concentration of CrkL-SH2 binding domains. Previously described binding partners to the CrkL-SH2 domain like CAS, DAB1, and DCBLD2 were identified in combination with a few new potential CrkL-SH2 binding partners.

DCBLD1, a homologue of the DCBLD2 receptor, was pulled out by the screen due to its 8 CrkL-SH2 binding motifs. The overall structure of the homologue is very similar to DCBLD2 and could allow it to function in a similar fashion. The two proteins share the same 3 extracellular domains and both have CrkL-SH2 binding motifs on their C-termini (Figure B1 A and B). To determine if DCBLD1 could act in a similar fashion to DCBLD2, biochemical characterization of the protein was undertaken.

The mouse isoform of Dcbld1 needed to be used in the biochemical classification of Dcbld1, because the human form of the protein could not be expressed properly in HEK293 cells. The mouse isoform lacks the entire FV/VIII domain (Figure B1 A) making it 200 amino acids smaller than DCBLD1 in human. Despite this domain loss the mouse form of the protein is still highly similar (Figure B1 A and B). With an extracellular domain and the YxxP CrkL-SH2 binding sites, the mouse form of Dcbld1

could potentially still function in the same manner as human DCBLD1 (Figure B1 A, B, and C).

The zebrafish work already underway required us to take a closer look at dcbld1 in zebrafish to ensure our knockdown was not being compromised. dcbld1 could potentially be compensating for the loss of dcbld1 and partially rescuing our knockdown. However, the zebrafish form of dcbld1did not share the conservation that the human forms of the protein did (Figure B1 A and B). The zebrafish dcbld1 is 270 amino acids, whereas human DCBLD1 is 715 (Figure B1 A and B). The zebrafish dcbld1 protein is essentially the outermost region of extracellular portion of the human form of DBCLD1. While the zebrafish form of the protein does have an extracellular CUB and FV/VIII domain, it lacks the LCCL domain and, most critically, does not have any YxxP CrkL-SH2 binding motifs (Figure B1 B).

The only data on dcbld1 in zebrafish is large scale *in situ* hybridizations. dcbld1 does show some nervous tissue staining (Figure S1), but it does not have the same patterning as dcbld2. Due to the lack of CrkL-SH2 binding sites in zebrafish dcbld1 and overall protein differences, we were fairly confident in assuming dcbld1 does not signal in the same way as dcbld2 in zebrafish. Therefore, we believe our knockdown was not being partially rescued by dcbld1compensation. It is important to note that we do not have empirical evidence supporting or refuting dcbld1's involvement in zebrafish nervous tissue development. More work will need to be completed to understand the function it has in zebrafish.

Materials and Methods

HEK 293 cells were grown in DMEM and underwent calcium phosphate transfection of 6 ug of *DCBLD2*-Flag or the *dcbld1*-FLAG as previously described (Aten, Redmond et al. 2013). Cells were stimulated with 8 mM with hydrogen peroxide for 20 minutes. Cells were lysed, as previously described (Aten, Redmond et al. 2013), and WCEs were blotted for α-Flag and α-pY. Lysates from hydrogen peroxide treated and untreated cells were rocked overnight at 4°C on a GST-CrkL-SH2 resin. Eluates from CrkL-SH2 resin were blotted for α-Flag.

Results and Discussion

Hydrogen peroxide-induced tyrosine phosphorylation in all treated cells (Figure B1 C). DCBLD2 was used as a control, as it had been previously shown to bind the CrkL-SH2 domain when stimulated via H_2O_2 (Aten, Redmond et al. 2013). H_2O_2 did lead to phosphorylation of both DCBLD2 and 1, and induced binding of the CrkL-SH2 domain to both isoforms of the receptor (Figure B1 C). While the overall level of DBCLD1 was higher in untreated cells, only the sample coming from hydrogen peroxide treated cells bound the GST-CrkL-SH2 resin (Figure B1 C). This indicates that phosphorylation of DCBLD1 induced by H_2O_2 was sufficient to cause the binding of the CrkL-SH2 domain.

While it was shown here that, similar to DCBLD2, Dcbld1 can bind the CrkL-SH2 domain when tyrosine phosphorylated, further work must be completed to fully characterize DCBLD1. Differential signaling between the two isoforms would be a

logical next step. If the proteins are able to interact with different binding partners downstream effectors may also differ and subsequent effects on the cell could vary. One way to approach the binding partner would be to use SILAC. Heavy and light isotopes would allow you to differentiate between the two samples and the proteins they interact with.

Lastly, the notion that the zebrafish dcbld1 was different enough in sequence and structure to have divergent function from dcbld2 would need to be confirmed. Because the zebrafish dcbld1 receptor is essentially a portion of the extracellular domain it could be dampening the effects of dcbld2, acting as a dominant negative. If the ligand for dcbld2 can also bind dcbld1 in zebrafish, you would assume some quantity of ligand is binding to dcbld1 and because the signal cannot be transduced via the CrkL adaptor protein, the signal would be diminished. This is assuming a similar signal transduction pathway. Zebrafish dcbld1 is very different and the research is so limited, it is difficult to assume any type of interaction with confidence.

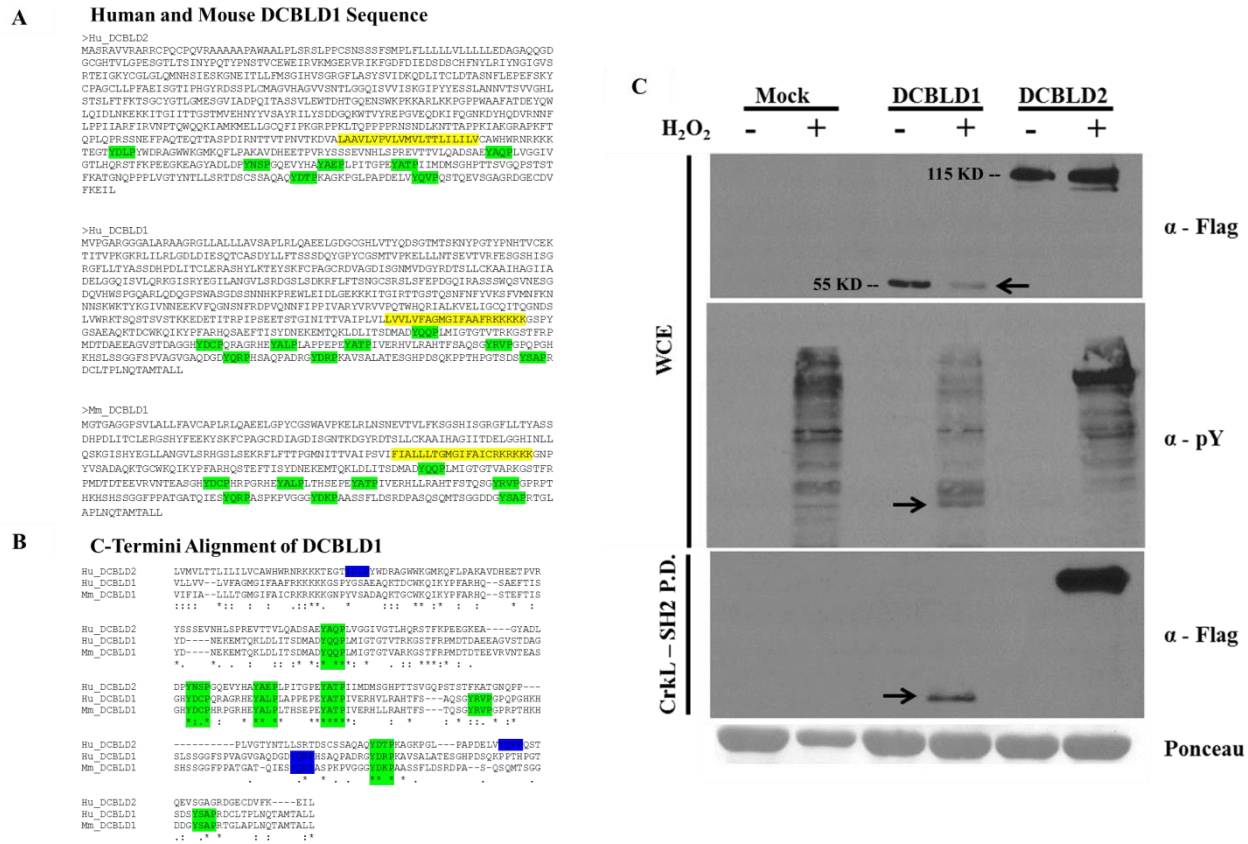

Figure B1. DCBLD1 has 8 YxxP CrkL-SH2 binding motifs and can bind the CrkL adaptor protein when tyrosine phosphorylated. Overall protein sequence of human and mouse DCBLD1 in comparison to human DCBLD2 (A). CrkL YxxP binding sites are highlighted in green and the transmembrane domain in yellow (A, B). Human and mouse DCBLD1, despite missing 200 amino acids in the FV/VIII domain, are 60.3% similar and 51% identical. C-terminus alignment of human and mouse DCBLD1 in comparison to human DCBLD2 (B), highlighting the presence of the CrkL-SH2 YxxP binding motifs (B). DCBLD1 is tyrosine phosphorylated (arrow) in response to H_2O_2 treatment (C). When phosphorylated, DCBLD1 can bind the CrkL-SH2 domain (arrow, C). DCBLD2, as a control, confirms H_2O_2 phosphorylation and binding to the CrkL-SH2 domain (C). Multiple sequence alignment was performed in Clustal Omega (Sievers, 2011 #1541).

Appendix C – SEMA4B is a Binding Partner of DCBLD2

Many of the proteins that regulate cellular migration during development have also been connected to the growth and metastasis of cancer. Semaphorin 4B (SEMA4B) is a transmembrane receptor that is involved in many developmental pathways including cell migration and regulation of axon extension (Nagai, Sugito et al. 2007). While investigating proteins involved in these processes, a group identified CLCP1 (DCBLD2) as being upregulated in a highly metastatic lunger cancer cell line (Nagai, Sugito et al. 2007). Knockdown of the DCBLD2 receptor resulted in reduced motility of the cancer cells (Nagai, Sugito et al. 2007). DCBLD2's neuropilin like structure led the group to test if the receptor bound any of the semaphoring family members.

By utilizing a phage display, in which peptide sequence libraries are cloned into position behind a phage coat protein, they were able to determine a binding sequence for DCBLD2 (Nagai, Sugito et al. 2007). The binding sequence identified matched a sequence in the SEMA4B SEMA domain (Nagai, Sugito et al. 2007). This was followed up by demonstration of DCBLD2 and SEMA4B co-immunoprecipitation and co-localization of the receptors at the membrane (Nagai, Sugito et al. 2007). Recapitulation of this study was necessary to confirm the DCBLD2 SEMA4B interaction and to investigate the tyrosine phosphorylation state of the receptors during the interaction.

Materials and Methods

A DCBLD2-Flag-Myc HEK293 stable cell line was created by selecting transfected cells that had taken up the plasmid and attained G418 antibiotic resistance.

SEMA4B-HA had to be shuttled, using gateway cloning as previously described (Petersen and Stowers 2011), into the PCC384 vector in order to place an HA tag on the protein and to put its expression under the control of a constitutive mammalian expression promoter. Wildtype or DCBLD2-Flag stably expressing HEK 293 cells were grown in DMEM and underwent calcium phosphate transfection of 5 ug of SEMA4B as previously described (Aten, Redmond et al. 2013). Cells were washed with warm DMEM after 6 hours transfection and then incubated for 12 more hours. Cell lysis and FLAG immunoprecipitations (FLAG-IP) were performed as previously described (Aten, Redmond et al. 2013). WCEs were blotted with α-HA and α-pY. The FLAG-IP was immunoblotted with α-HA. FYN was transfected in as a positive control for inducing DCBLD2 phosphorylation. SOS-HA (+) was also transfected into cells to ensure the HA tag and detecting antibody were functioning properly.

In an attempt to allow the extracellular domains of DCBLD2 and SEMA4B to interact, multiple binding trials were executed. SEMA4B was initially transfected in to DCBLD2 stably expressing cells. SEMA4B was also transfected into WT HEK293 cells. The transfected cells were then detached from the dish with trypsin and plated directly on the stable cell line. Cells were allowed to adhere and interact for 4 hours. The reciprocal was also completed; using trypsin to detach stably expressing DCBLD2 cells and then plating them on top of SEMA4B transfected cells.

Results and Discussion

An α-HA blot on WCE confirmed that SEMA4B cloning had been successful and

the receptor was being produced under the constitutive promoter (Figure C1 A). However, neither DCBLD2 or SEMA4B were phosphorylated as a result of their interaction (Figure C1 B). DCBLD2 and SEMA4B did co-immunoprecipitate in the FLAG-IP (Figure C1 C). However, this was again not a result of phosphorylation of either receptor (Figure C1 D). Overexpressed FYN phosphorylated DCBLD2 in the stable cell line throughout the experiment (Figure C1 B and D), leaving us confident that the receptors were not being phosphorylated as a result of their interaction.

DCBLD2 needs to tyrosine phosphorylated in order to interact with the CrkL-SH2 domain. So while it is clear the DCBLD2 and SEMA4B do interact, their mechanism of function is not likely to be routed through CrkL adaptor protein, or at least not directly. The data collected confirmed the previous research that the two receptors interact, however, this interaction is not yet understood from a functional perspective. The group claims that the DCBLD2 SEMA4B interaction results in ubiquitination of DCBLD2 and degradation by the proteasome (Nagai, Sugito et al. 2007). Increased expression of DCBLD2 in the metastatic lung cancer cell line led to increased motility of cells, and so the overall conclusion was that SEMA4B negatively regulates DCBLD2 expression and therefore cell motility (Nagai, Sugito et al. 2007).

The interaction between DCBLD2 and SEMA4B does seem to be regulatory in nature. While this was not the expected result, it allowed us to learn more about the receptor. Not every interaction is phosphotyrosine dependent and this would allow the receptor to have differential signaling capability as was predicted. More work needs to be completed to fully characterize the signals DCBLD2 responds to and how those signals

affect cellular changes or mediate processes.

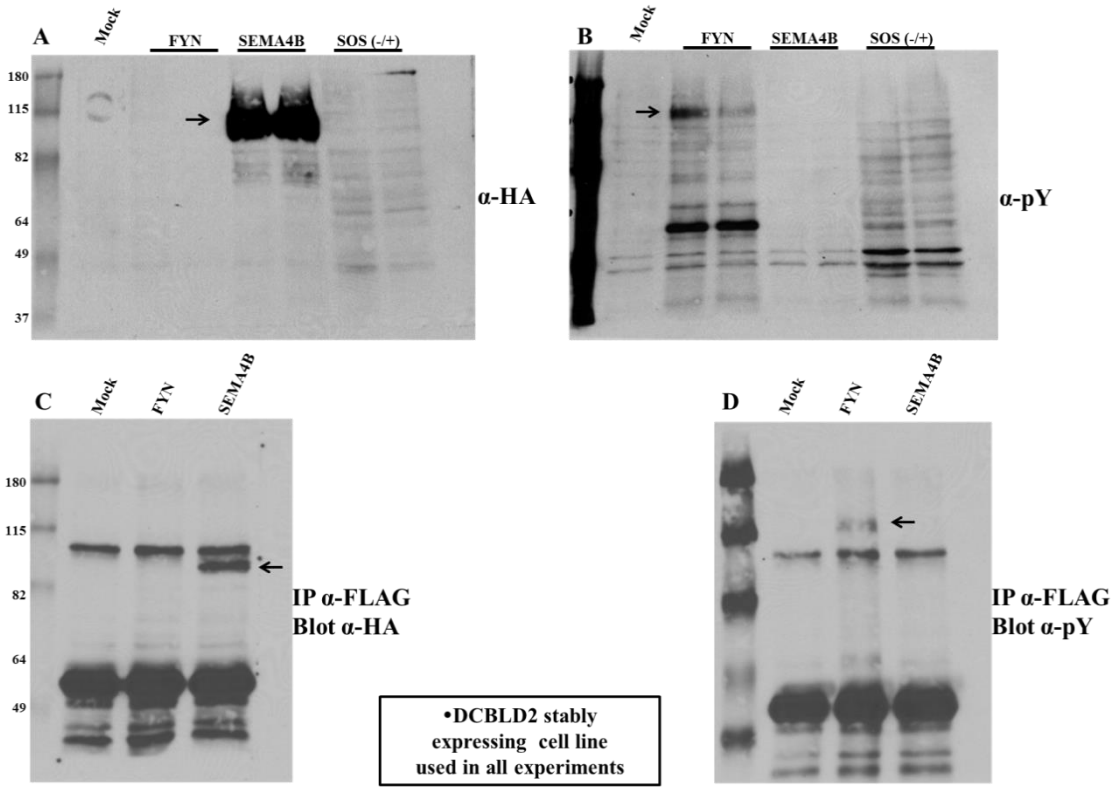

Figure C1. DCBLD2 and SEMA4B interact, but their association is not tyrosine phosphorylation dependent. SEMA4B (arrow) is expressed strongly in HEK293 cells and the HA-tag and antibody function properly (A). FYN, but not SEMA4B, results in tyrosine phosphorylation of DCBLD2 receptor (arrow, B and D). DCBLD2 and SEMA4B (arrow) co-immunoprecipitate in α-FLAG IP (C). The interaction of DCBLD2 and SEMA4B does not result in tyrosine phosphorylation of either receptor, even when lysates are enriched via FLAG-IP (D).

SUPPLEMENTAL FIGURES

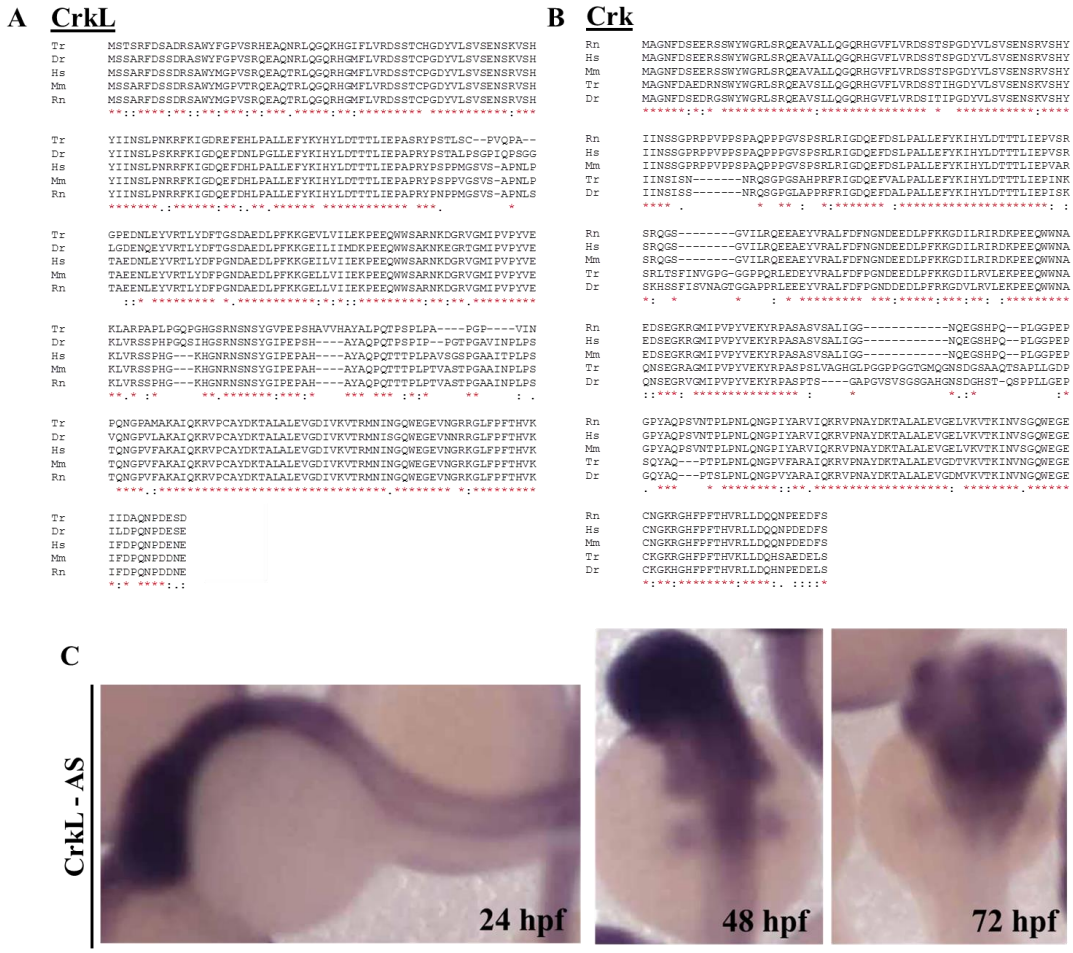

Figure S1. Crk and CrkL adaptor proteins are well conserved across taxa. Both CrkL (71.38%) and Crk (63.5%) are highly conserved from puffer fish to rat (A and B). The available *in situ* hybridization data shows that CrkL has a similar neuraonal staining pattern, with strong expression in the developing nervous tissue (C). Panel C adapted from Thisse, Heyer et al. 2004. Multiple sequence alignment was performed in Clustal Omega (Sievers, Wilm et al. 2011).

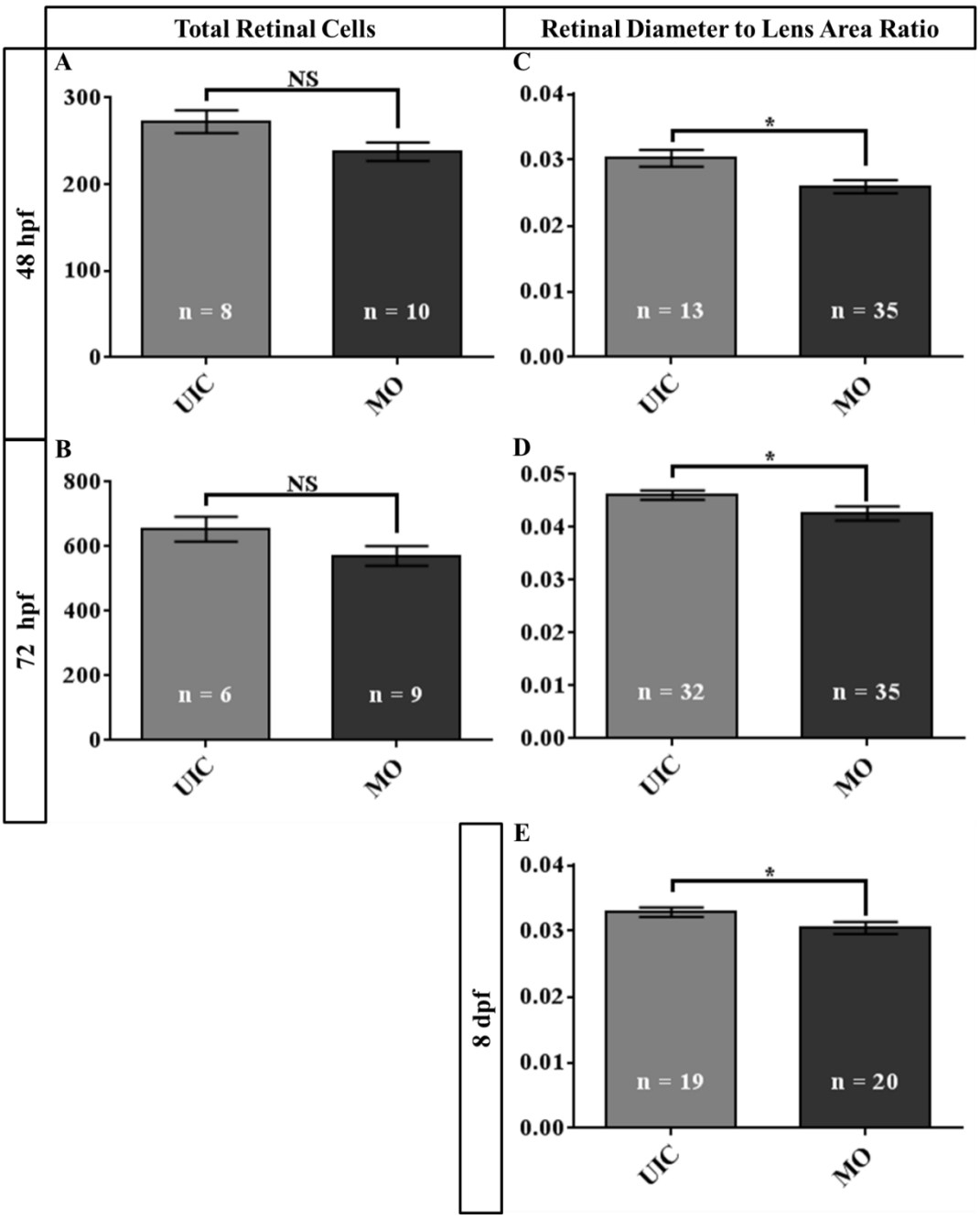

Figure S2. Morphants do not have a reduced number of precursor cells, but form smaller retinas relative to the lens. Morphant fish show a non-significant difference in total retinal precursor cells at 48 and 72 hpf (A and B, P>0.05, unpaired Students t-test). Retinal diameter to lens ratio supports retinas are specifically reduced in size without size change in the lens, which derives from a different parent tissue (C, D, and E, P<0.05, unpaired Student's t-test).

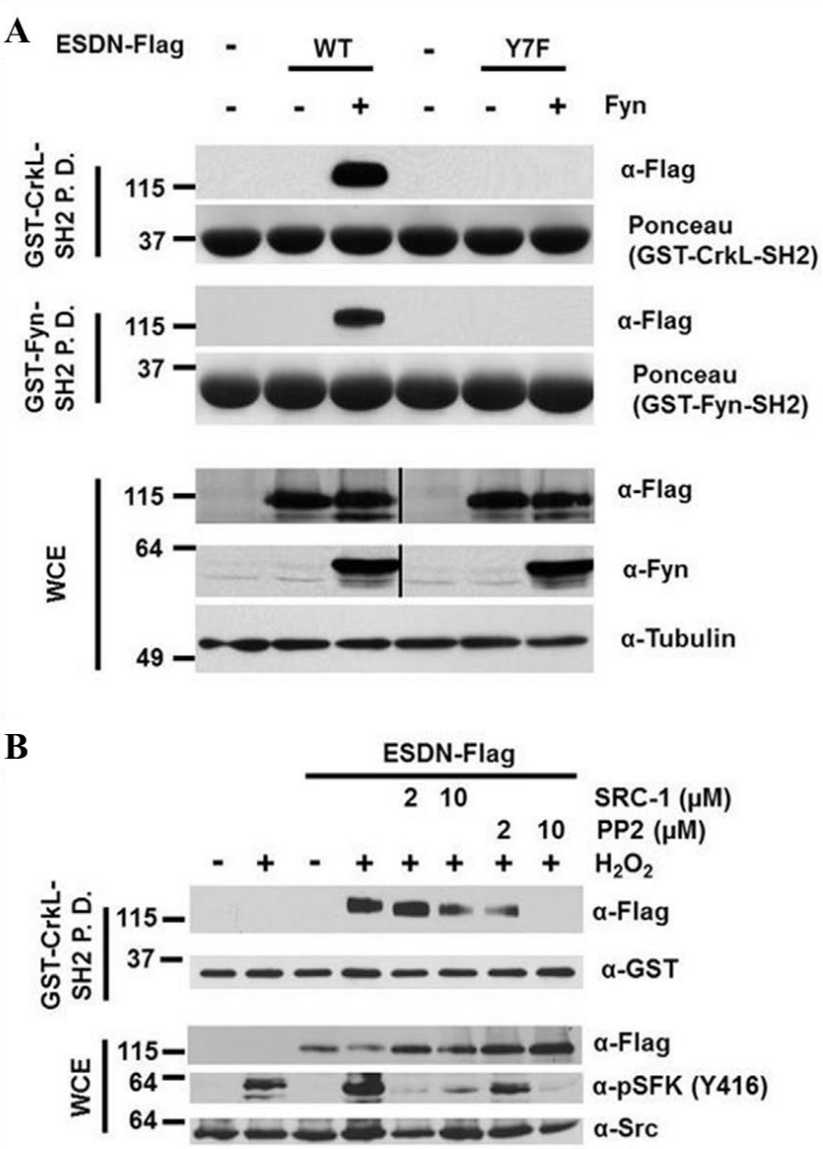

Figure S3. SFKs can facilitate the interaction between DCBLD2/ESDN and the CrkL-SH2 domain. The SFK, FYN, can facilitate the interaction of DCBLD2 and the CrkL-SH2 domain (A). A general kinase inhibitor and a highly specific SFK inhibitor demonstrate that while SFKs are sufficient to induce binding of DCBLD2/ESDN to the CrkL-SH2 domain, they are not necessary (B). Adapted from Aten, Redmond et al. 2013.

Bibliography

Andermann, P., J. Ungos and D. W. Raible 2002. Neurogenin1 defines zebrafish cranial sensory ganglia precursors. Dev Biol 251(1): 45-58.

Appel, B., L. A. Givan and J. S. Eisen 2001. Delta-Notch signaling and lateral inhibition in zebrafish spinal cord development. BMC Dev Biol 1: 13.

Arnaud, L., B. A. Ballif, E. Forster and J. A. Cooper 2003. Fyn tyrosine kinase is a critical regulator of disabled-1 during brain development. Curr Biol 13(1): 9-17.

Aten, T. M., M. M. Redmond, S. O. Weaver, C. C. Love, R. M. Joy, A. S. Lapp, O. D. Rivera, K. L. Hinkle and B. A. Ballif 2013. Tyrosine phosphorylation of the orphan receptor ESDN/DCBLD2 serves as a scaffold for the signaling adaptor CrkL. FEBS Lett 587(15): 2313-2318.

Ballif, B. A., L. Arnaud, W. T. Arthur, D. Guris, A. Imamoto and J. A. Cooper 2004. Activation of a Dab1/CrkL/C3G/Rap1 pathway in Reelin-stimulated neurons. Curr Biol 14(7): 606-610.

Bill, B. R., A. M. Petzold, K. J. Clark, L. A. Schimmenti and S. C. Ekker 2009. A primer for morpholino use in zebrafish. Zebrafish 6(1): 69-77.

Bork, P. and G. Beckmann 1993. The CUB domain. A widespread module in developmentally regulated proteins. J Mol Biol 231(2): 539-545.

Brand, M., M. Granato and C. Nüsslein-Volhard 2002. Keeping and raising zebrafish. Zebrafish 261: 7-37.

Brown, K. E., P. J. Keller, M. Ramialison, M. Rembold, E. H. Stelzer, F. Loosli and J. Wittbrodt 2010. Nlcam modulates midline convergence during anterior neural plate morphogenesis. Dev Biol 339(1): 14-25.

Catalano, A. E., P. A. Raymond, D. Goldman and X. Wei 2007. Zebrafish dou yan mutation causes patterning defects and extensive cell death in the retina. Dev Dyn 236(5): 1295-1306.

Cavodeassi, F., F. Carreira-Barbosa, R. M. Young, M. L. Concha, M. L. Allende, C. Houart, M. Tada and S. W. Wilson 2005. Early stages of zebrafish eye formation require the coordinated activity of Wnt11, Fz5, and the Wnt/beta-catenin pathway. Neuron 47(1): 43-56.

Chang, K. T. and K. T. Min 2011. Progress in molecular biology and translational science. Animal models of human disease. Preface. Prog Mol Biol Transl Sci 100: xv.

Dievler, A. 1997. Fighting tuberculosis in the 1990s: how effective is planning in policy making? J Public Health Policy 18(2): 167-187.

Ekker, S. C. and J. D. Larson 2001. Morphant technology in model developmental systems. Genesis 30(3): 89-93.

Feller, S. M. 2001. Crk family adaptors-signalling complex formation and biological roles. Oncogene 20(44): 6348-6371.

Feng, H., G. Y. Lopez, C. K. Kim, A. Alvarez, C. G. Duncan, R. Nishikawa, M. Nagane, A. J. Su, P. E. Auron, M. L. Hedberg, L. Wang, J. J. Raizer, J. A. Kessler, A. T. Parsa, W. Q. Gao, S. H. Kim, M. Minata, I. Nakano, J. R. Grandis, R. E. McLendon, D. D. Bigner, H. K. Lin, F. B. Furnari, W. K. Cavenee, B. Hu, H. Yan and S. Y. Cheng 2014. EGFR phosphorylation of DCBLD2 recruits TRAF6 and stimulates AKT-promoted tumorigenesis. J Clin Invest 124(9): 3741-3756.

Fuhrmann, S. 2008. Wnt signaling in eye organogenesis. Organogenesis 4(2): 60-67.

Gale, N. W. and G. D. Yancopoulos 1999. Growth factors acting via endothelial cell-specific receptor tyrosine kinases: VEGFs, angiopoietins, and ephrins in vascular development. Genes Dev 13(9): 1055-1066.

Gibson, J. (2014). Development through Seasonal Worker Programs The Case of New Zealand's RSE Program. [S.l.], World Bank, Washington, DC.

Guo, X., L. Nie, L. Esmailzadeh, J. Zhang, J. R. Bender and M. M. Sadeghi 2009. Endothelial and smooth muscle-derived neuropilin-like protein regulates platelet-derived growth factor signaling in human vascular smooth muscle cells by modulating receptor ubiquitination. J Biol Chem 284(43): 29376-29382.

Jensen, L. J., M. Kuhn, M. Stark, S. Chaffron, C. Creevey, J. Muller, T. Doerks, P. Julien, A. Roth, M. Simonovic, P. Bork and C. von Mering 2009. STRING 8--a global view on proteins and their functional interactions in 630 organisms. Nucleic Acids Res 37(Database issue): D412-416.

Jossin, Y. and J. A. Cooper 2011. Reelin, Rap1 and N-cadherin orient the migration of multipolar neurons in the developing neocortex. Nat Neurosci 14(6): 697-703.

Karlsson, J., J. von Hofsten and P. E. Olsson 2001. Generating transparent zebrafish: a refined method to improve detection of gene expression during embryonic development. Mar Biotechnol (NY) 3(6): 522-527.

Keane, M. M., O. M. Rivero-Lezcano, J. A. Mitchell, K. C. Robbins and S. Lipkowitz 1995. Cloning and characterization of cbl-b: a SH3 binding protein with homology to the c-cbl proto-oncogene. Oncogene 10(12): 2367-2377.

Kennedy, B. N., G. W. Stearns, V. A. Smyth, V. Ramamurthy, F. van Eeden, I. Ankoudinova, D. Raible, J. B. Hurley and S. E. Brockerhoff 2004. Zebrafish rx3 and mab21l2 are required during eye morphogenesis. Dev Biol 270(2): 336-349.

Kimmel, C. B., W. W. Ballard, S. R. Kimmel, B. Ullmann and T. F. Schilling 1995. Stages of embryonic development of the zebrafish. Dev Dyn 203(3): 253-310.

Kobuke, K., Y. Furukawa, M. Sugai, K. Tanigaki, N. Ohashi, A. Matsumori, S. Sasayama, T. Honjo and K. Tashiro 2001. ESDN, a novel neuropilin-like membrane protein cloned from vascular cells with the longest secretory signal sequence among eukaryotes, is up-regulated after vascular injury. J Biol Chem 276(36): 34105-34114.

Kruger, R. P., J. Aurandt and K. L. Guan 2005. Semaphorins command cells to move. Nat Rev Mol Cell Biol 6(10): 789-800.

Lakshmikanthan, S., M. Sobczak, C. Chun, A. Henschel, J. Dargatz, R. Ramchandran and M. Chrzanowska-Wodnicka 2011. Rap1 promotes VEGFR2 activation and angiogenesis by a mechanism involving integrin alphavbeta(3). Blood 118(7): 2015-2026.

Lemmon, M. A. and J. Schlessinger 2010. Cell signaling by receptor tyrosine kinases. Cell 141(7): 1117-1134.

Malicki, J., H. Jo and Z. Pujic 2003. Zebrafish N-cadherin, encoded by the glass onion locus, plays an essential role in retinal patterning. Dev Biol 259(1): 95-108.

Nagai, H., N. Sugito, H. Matsubara, Y. Tatematsu, T. Hida, Y. Sekido, M. Nagino, Y. Nimura, T. Takahashi and H. Osada 2007. CLCP1 interacts with semaphorin 4B and regulates motility of lung cancer cells. Oncogene 26(27): 4025-4031.

Nie, L., X. Guo, L. Esmailzadeh, J. Zhang, A. Asadi, M. Collinge, X. Li, J. D. Kim, M. Woolls, S. W. Jin, A. Dubrac, A. Eichmann, M. Simons, J. R. Bender and M. M. Sadeghi 2013. Transmembrane protein ESDN promotes endothelial VEGF signaling and regulates angiogenesis. J Clin Invest 123(12): 5082-5097.

O'Connor, M. N., Salles, II, A. Cvejic, N. A. Watkins, A. Walker, S. F. Garner, C. I. Jones, I. C. Macaulay, M. Steward, J. J. Zwaginga, S. L. Bray, F. Dudbridge, B. de Bono, A. H. Goodall, H. Deckmyn, D. L. Stemple, W. H. Ouwehand and C. Bloodomics 2009. Functional genomics in zebrafish permits rapid characterization of novel platelet membrane proteins. Blood 113(19): 4754-4762.

Palmer, A. and R. Klein 2003. Multiple roles of ephrins in morphogenesis, neuronal networking, and brain function. Genes Dev 17(12): 1429-1450.

Park, T. J. and T. Curran 2008. Crk and Crk-like play essential overlapping roles downstream of disabled-1 in the Reelin pathway. J Neurosci 28(50): 13551-13562.

Petersen, L. K. and R. S. Stowers 2011. A Gateway MultiSite recombination cloning toolkit. PLoS One 6(9): e24531.

Peterson, S. M. and J. L. Freeman 2009. RNA isolation from embryonic zebrafish and cDNA synthesis for gene expression analysis. J Vis Exp(30).

Pittman, A. J., M. Y. Law and C. B. Chien 2008. Pathfinding in a large vertebrate axon tract: isotypic interactions guide retinotectal axons at multiple choice points. Development 135(17): 2865-2871.

Poggi, L., M. Vitorino, I. Masai and W. A. Harris 2005. Influences on neural lineage and mode of division in the zebrafish retina in vivo. J Cell Biol 171(6): 991-999.

Robu, M. E., J. D. Larson, A. Nasevicius, S. Beiraghi, C. Brenner, S. A. Farber and S. C. Ekker 2007. p53 activation by knockdown technologies. PLoS Genet 3(5): e78.

Sadeghi, M. M., L. Esmailzadeh, J. Zhang, X. Guo, A. Asadi, S. Krassilnikova, H. R. Fassaei, G. Luo, R. S. Al-Lamki, T. Takahashi, G. Tellides, J. R. Bender and E. R. Rodriguez 2007. ESDN is a marker of vascular remodeling and regulator of cell proliferation in graft arteriosclerosis. Am J Transplant 7(9): 2098-2105.

Sernagor, E. 2006. Retinal development. Cambridge, Cambridge University Press.

Sievers, F., A. Wilm, D. Dineen, T. J. Gibson, K. Karplus, W. Li, R. Lopez, H. McWilliam, M. Remmert, J. Soding, J. D. Thompson and D. G. Higgins 2011. Fast, scalable generation of high-quality protein multiple sequence alignments using Clustal Omega. Mol Syst Biol 7: 539.

Smolen, G. A., B. J. Schott, R. A. Stewart, S. Diederichs, B. Muir, H. L. Provencher, A. T. Look, D. C. Sgroi, R. T. Peterson and D. A. Haber 2007. A Rap GTPase interactor, RADIL, mediates migration of neural crest precursors. Genes Dev 21(17): 2131-2136.

Stadler, J. A., A. Shkumatava and C. J. Neumann 2004. The role of hedgehog signaling in the development of the zebrafish visual system. Dev Neurosci 26(5-6): 346-351.

Stork, P. J. and T. J. Dillon 2005. Multiple roles of Rap1 in hematopoietic cells: complementary versus antagonistic functions. Blood 106(9): 2952-2961.

Sullivan-Brown, J., M. E. Bisher and R. D. Burdine 2011. Embedding, serial sectioning and staining of zebrafish embryos using JB-4 resin. Nat Protoc 6(1): 46-55.

Thisse, B., V. Heyer, A. Lux, V. Alunni, A. Degrave, I. Seiliez, J. Kirchner, J. P. Parkhill and C. Thisse 2004. Spatial and temporal expression of the zebrafish genome by large-scale in situ hybridization screening. Methods Cell Biol 77: 505-519.

Trexler, M., L. Banyai and L. Patthy 2000. The LCCL module. Eur J Biochem 267(18): 5751-5757.

Vogel, W. F., R. Abdulhussein and C. E. Ford 2006. Sensing extracellular matrix: an update on discoidin domain receptor function. Cell Signal 18(8): 1108-1116.

Wang, H. U., Z. F. Chen and D. J. Anderson 1998. Molecular distinction and angiogenic interaction between embryonic arteries and veins revealed by ephrin-B2 and its receptor Eph-B4. Cell 93(5): 741-753.

Yuan, Z. M., Y. Huang, T. Ishiko, S. Kharbanda, R. Weichselbaum and D. Kufe 1997. Regulation of DNA damage-induced apoptosis by the c-Abl tyrosine kinase. Proc Natl Acad Sci U S A 94(4): 1437-1440.

Zou, S. Q., W. Yin, M. J. Zhang, C. R. Hu, Y. B. Huang and B. Hu 2010. Using the optokinetic response to study visual function of zebrafish. J Vis Exp(36).

Zuber, M. E., G. Gestri, A. S. Viczian, G. Barsacchi and W. A. Harris 2003. Specification of the vertebrate eye by a network of eye field transcription factors. Development 130(21): 5155-5167.